RESERVOIR CHARACTERIZATION OF LOWER GORU SANDS AT MIANO AREA USING MODEL BASED INVERSION TECHNIQUE, CENTRAL INDUS BASIN, PAKISTAN

ANAM SHER JANJUA
01-262162-004

A thesis submitted in fulfilment of the requirements for the award of the degree of Masters of Sciences (Geophysics)

Department of Earth and Environmental Sciences

Bahria University, Islamabad

August 2020

[redacted]

ces

tal

he

Committee Member	Name	Signature
		
		
		
		

Dr. Said Akbar Khan
(E&ES)

Approval for Examination

Scholar's Name: _____ Registration No. _____

Programme of Study:

_____

_____

Thesis Title:

_____

_____

_____

It is to certify that the above scholar's thesis has been completed to my satisfaction and, to my belief, its standard is appropriate for submission for examination. I have also conducted plagiarism test of this thesis using HEC prescribed software and found similarity index _____% that is within the permissible limit set by the HEC for the PhD degree thesis. I have also found the thesis in a format recognized by the BU for the PhD thesis.

Principal Supervisor's Signature:

_____

Date: _____

Name: _____

Author's Declaration

I, _____ hereby state that my MS thesis titled "_____
_____
_____" is my own work and has not been submitted previously by me for taking any degree from this university is my own work and has not been submitted previously by me for taking any degree from this university_____ (Name of University)_____or anywhere else in the country/world.

At any time if my statement is found to be incorrect even after my graduation, the University has the right to withdraw/cancel my MS degree.

Name of scholar: _____

Date: _____

Plagiarism Undertaking

I, solemnly declare that research work presented in the thesis titled "_____ _____ _____"

is solely my research work with no significant contribution from any other person. Small contribution / help wherever taken has been duly acknowledged and that complete thesis has been written by me.

I understand the zero tolerance policy of the HEC and Bahria University towards plagiarism. Therefore I as an Author of the above titled thesis declare that no portion of my thesis has been plagiarized and any material used as reference is properly referred / cited.

I undertake that if I am found guilty of any formal plagiarism in the above titled thesis even after award of MS degree, the university reserves the right to withdraw / revoke my PhD degree and that HEC and the University has the right to publish my name on the HEC / University website on which names of scholars are placed who submitted plagiarized thesis.

Scholar / Author's Sign: _____

Name of the Scholar: _____

DEDICATION

I want to express my thanks and gratitude to my parents for their immense support throughout this research especially and through every stage of my life. May Allah keep them under his protection and blessings, always.

ACKNOWLEDGEMENTS

All gestures of recognition and appreciation to Allah Almighty who favored me with the capacity and inspiration to come up with this research paper. An extremely genuine and sincere thanks to my supervisor Dr. Fahad Mehmood, Assistant Professor at Department of Earth and Environmental Sciences, Bahria University, Islamabad. He gave me all the important direction and good help, being dependably there for me, to help and make things reasonable and simpler to guarantee the completion of my research work in time. I likewise owe a special thanks to my co-supervisor Dr. Muhammad Zahid Afzal Durrani, Rock Physics Specialist at Exploration Department, Pakistan Petroleum Limited (PPL) for his guidance and much valued suggestions for my work which helped me improve my research work better. In addition, I was fortunate enough that Prof. Dr. Muhammad Zafar and Head of Department Dr. Tahseenullah Khan, Department of Earth and Environmental Sciences, Bahria University, Islamabad, took out their time to review my thesis and added to the nature of work introduced in this research. I cannot forget to thank my seniors and friends, Aqsa Afzal (Quaid-e-azam University), Beenish Aslam (Bahria University) and Ammad (Bahria University) for all their assistance and guidance. Lastly, I would like to acknowledge Directorate General of Petroleum Concession (DGPC) for providing geophysical and geological data, the teams of SMT Kingdom and Geographix software's for providing handy and useful tools which helped me in carrying out my research work

ABSTRACT

Fields that are significantly producing hydrocarbons in the Central Indus Basin has Miano in the category too. Real goal of this exploration was to describe the reservoir potential and to further exploit the reservoirs of Lower Goru B Sands. These channel sands dependably put a challenge before geoscientists to exploit the reservoirs that are channeled in such a territory for the assessment of hydrocarbon potential. To determine this issue, this exploration work uses the advanced seismic methods like seismic inversion and seismic attribute analysis alongside the help of seismically interpreting and petrophysical examination of Miano region, Pakistan. The available data helps in defining the physical attributes of the reservoir with the help of certain types of modelling techniques. The simulated behavior of fluids in reservoir modelling provide a head start to the Exploration and Production companies to progress their optimal production techniques. Not one but different geophysical techniques are brought into use to attain accurately characterized reservoirs, including the correlation of the results. At the level of Lower Goru B Sands negative flower structure (strike slip component) is observed. At the level of Lower Goru B Sands fault blocks that are tilted in NE-SW orientation with a two-way dip closure exists. Horsts graben structures are also observed at the level of Lower Goru B Sands. In compartmentalizing the reservoir, NW-SE trending faults plays a fundamental role. Petrophysical investigation demonstrated that at least one reservoir zone having sufficient thickness and hydrocarbon saturation in each Miano well is possibly sufficiently stable to deliver at commercial level. Comparison of different frequency ranges with

Lower Goru B Sands response was made using spectral decomposition, the response indicated inverse relation between frequency and sand beds thickness. Using spectral decomposition clear zones of sand bodies having channeled geometries are stipulated. Bright spots are marked with the help of instantaneous amplitude attribute at Lower Goru B Sands hence making it a potential reservoir zone of Miano area. Different seismic inversion methods based on acoustic impedance variation over the investigation region and porosity calculation unmistakably upgraded the sweet spots eastbound way at Lower Goru B Sands level which is solid for encouraging improvement of this field.

TABLE OF CONTENTS

LIST OF TABLES

LIST OF FIGURES

CHAPTER 1

INTRODUCTION

Assurance of petrophysical parameters utilizing accessible information particularly important in exploration and production study in the industry. For instance, assessing of corrected porosity as a petrophysical parameter can aid in making high budgetary risk decisions, for example, deciding regarding drilling. In this way, the investigation of seismic information, seismic attribute extraction from them and incorporating the extracted attributes by well log data is a critical key for discovery of properties of reservoir. Acoustic impedance is an important framework for making seismic interpretation and first hand geologic interpretation and for detecting lateral lithologic variation. Product of density and velocity characterizes acoustic impedance. Seismic inversion is utilized to gauge detailed seismic and rock properties, for example, by using seismic data to take out acoustic impedance and porosity. The strategy is broadly utilized and demonstrated effective by the oil industry yet has so far not generally been embraced for scholarly investigations. Acoustic impedance information and the derived porosity distribution encourages itemized investigations of certain properties in the shallow subsurface namely lithology, compaction, and fluid flow all results by an examination of reflection and impedance information. Upon comparing the impedance and reflection data it is evidenced that the rise of seismic reflection events is a result of hitting the bed boundaries rather than the changes in impedance laterally. The seismic impedance results in a profile that depicts the changes in porosity and acoustic impedance along the wells (Soleimani et al., 2020)

Early 1970's mark the introduction of seismic attributes however now they have turned out to be an immensely important part of projects that are related to seismic interpretation (Chopra and Marfurt, 2006). Seismic attribute analysis is performed to gauge our seismic interpretation and provide us with a thoroughly detailed data to a seismic data interpretation in regards to stratigraphic, structural and lithological framework of the seismic prospect that leads the interpreter to hydrocarbon prospect identification and characterization of the reservoir. Conventional seismic interpretation results in subtle information regarding geological and geophysical information of an area and so interpretation is done accordingly, however seismic attribute analysis enhances the very same information resulting in an efficient and better interpretation (Taner, 2001).

1.1 Introduction to study area

The gas field namely Miano is situated in the Central Indus Basin, encompassing a total area of 814 sq.km, bounded by coordinates 27.10° N to 27.38° N latitude and 69.27°E to 69.50°E longitude. The area is located in Taluka Saleh Pat, District Sukkur of Sindh Province, Pakistan. Miano area comprises three union councils that are Saleh Pat, Tarai and Lal Jurio Shambani. The Miano gas field is found roughly 80 kms south of Sukkur in the Sindh Province, Pakistan. The discovery of Miano field dates to 1993. The gas field is a part of Central Indus Basin. The delivered gas is dry and condensate drop out is almost equivalent to none during the whole field life. Pakistan's two largest gas fields namely Mari and Sui gas fields are situated 75 km to the north respectively. Miano constitutes part of the Block 20 (concession map) which lies in the northern part of Lower Indus basin. The block extends from southern block boundary of Central Indus Basin to the northern direction. The fundamental reservoirs are the Lower Goru sands and from within lower Goru sands, B sands being the primary target whereas A sands as secondary target.

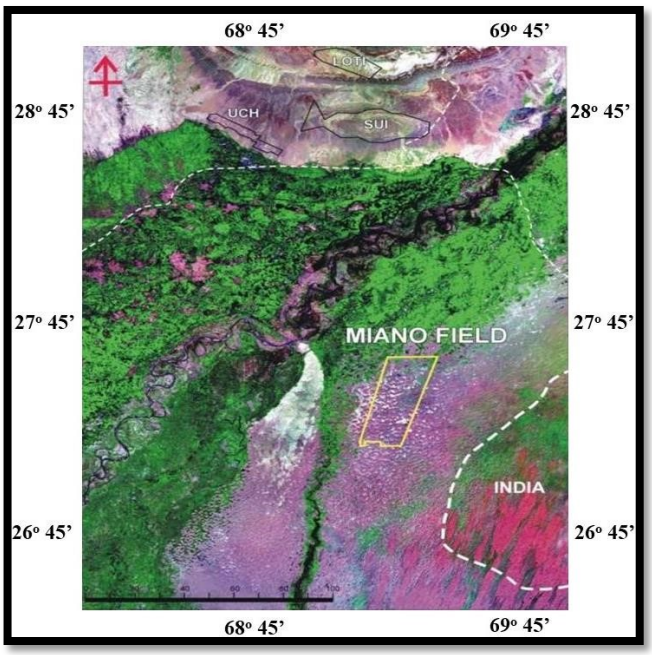

Figure 1.1. Landsat image showing Miano Field marked by yellow polygon (Bregar et al., 2008)

Currently OMV, ENI Pakistan Limited, Oil and Gas Development Company Limited OGDCL and Pakistan Petroleum Limited PPL are the operators in the development and production of Miano with a working interest of 17.68%, 15.16%, 52% and 15% respectively. The area of interest is gas prone and the traps appear to be structural as well as stratigraphic. (Currently OMV, ENI Pakistan Limited, Oil and Gas Development Company Limited OGDCL and Pakistan Petroleum Limited PPL are the administrators in the expansion, development and fair production of Miano bearing a working profit of 17.68%, 15.16%, 52% and 15% separately. The region under scrutiny is gas inclined and the traps have all the earmarks of being structural and in addition stratigraphic.

1.2 Exploration History

The first ever seismic survey was conducted by OMV in the Miano gas field. Currently, there exists 7 wells that are in the producing stage with the gas production rate of 120 million standard cubic feet of gas per day (Berger et al., 2008). The Miano gas field was announced to have first significant stratigraphic traps discovered. The Lower Goru Formation of Cretaceous age was targeted and later about 15 wells were drilled in pursuit to appraise the Miano field. The Lower Goru Formation of Miano gas field was drilled, containing combination of structural as well as stratigraphic traps. OMV is the primary operator of the Miano gas field, however partner companies include Pakistan Petroleum Limited (PPL), Eni and OGDCL (PPL annual report, 2011). 3-D seismic surveys were also carried out in the area for better resolution of the subsurface image, accurate identification of prospect of hydrocarbon and to enhance the production from traps that are stratigraphic in nature (Bregar et al., 2008).

1.3 Accessibility to the Area

The zone under investigation is connected by metaled and earthy roads from Sukkur (Krios et al., 1998). In total there are three streets that go to Miano area namely Thari Naro Street, Sanghar Street and Sawan Airport Street. Sand dunes portray the area's territory, adjusted NE-SW in the east and developed region in the western part. The normal stature of sand rises is around 50m in the south of the investigation zone and has the more extreme southern incline than the northern side.

1.4 Climate

Situated in a subtropical locale, Sindh is sweltering in the summers and cool in winter. Temperature every now and again transcend 46 degrees Celsius amongst May and August, and the base normal temperature of 2 degrees Celsius happens amid December and January. The yearly precipitation midpoints around seven inches, falling fundamentally amid July and August. The Southwest

monsoon winds starts to blow in mid-February and proceeds until the finish of September, though the cool northerly breeze blows amid the winter a long time from October to January.

1.5 Problem statement

As both types of traps are observed namely structural as well as stratigraphic, so to counter stratigraphic traps better, impedance data is better than seismic data. One of the major benefits of seismic inversion is substantial enhancement in the seismic resolution (Veeken, 2007) hence the choice.

The goal of the modern seismic interpretation has been extended to incorporate the extraction of the acoustic impedance contrast of the reflection rather than the conventional continuity of the horizon for structural interpretation. Assessment of selected seismic attributes applied on seismic data to confirm our structural interpretation, enhanced visualization of changes in lithology for reservoir channel characterization, detection of faults and identification of direct hydrocarbon indicators to establish and highlight any noteworthy relationship between attributes with producing field.

Quantification of geological rock properties like porosity, water saturation and hydrocarbon saturation of a well demands tools like wire line logging and petrophysical analysis. Extraction of these properties past the well control is fundamentally a matter of concern. We know that quantitative seismic interpretation is far better than conventional one in terms of accuracy and resolution. Besides, it is additionally the need of time to identify stratigraphic traps thoroughly as well.

1.6 Objectives

The main purpose of the study is to evaluate hydrocarbon potential of the area and to probe the potential of sands of Lower Goru Formation by utilizing seismic inversion, attribute analysis and Petrophysical techniques. This is done by interpreting the available seismic lines structurally. This structural and reservoir study reflected an idea about the favorable spots of hydrocarbon accumulation, which is the key part of objectives. The core objectives of dissertation are:

1. Seismic interpretation and mapping of study area for subsurface structural evaluation

2. Petrophysical interpretation of the reservoir formations to study the formation character

3. Attribute analysis to study the changes lithological changes, changes in reservoir thickness and presence of bright spots

4. Model based seismic inversion for the calculations of impedance and porosity evaluation at reservoir level

1.7 Available Dataset

Following public domain data was approved from DGPC and acquired from LMKR, on behalf of recommendation letter from the E&ES Department Bahria University, to achieve the desired research objectives.

1.7.1 Seismic lines

This research work plans to influence the peruser to comprehend the different steps that are engaged with seismic reflection interpretation and relationship of the outcomes which are gotten by the assistance of the seismic data with well logs, so a genuine basic model of the area under study can be

developed, likewise it expects to inspect the geological and geophysical properties like porosity and so forth to enable develop a comprehension about the capacity of the reservoir rock and would further develop the field. A total of seven seismic lines were given for seismic interpretation by LMKR, after endorsement from DGPC (Directorate General of Petroleum Concessions) to get data present in public domain. Lines in particular are P2092-110, P2092-113, P2092-115, P2092-117, P2092-119, P2092-121, and P2092-123. These lines are in view in the base map in figure 1.2. Amid these lines SP2092-110 is a strike line and whatever is left of them are dip lines. Well log information of three wells in particular Miano-03, Miano-04 and Miano-09 is utilized in this study. These wells are likewise shown in the base map in figure 1.1. Petrophysical understanding was attained with the assistance of Caliper log, GR log, Resistivity log, SP log, sonic log, Porosity log and Density log. SEG-Y's of seismic lines (Table 1.1) were attained for study purposes.

Table 1.1. Seismic lines required for the research work.

Line Name	**Orientation**
P2092-110	Strike
P2092-113	Dip
P2092-115	Dip
P2092-117	Dip
P2092-119	Dip
P2092-121	Dip
P2092-123	Dip

1.7.2 Well data

Wireline logs (Gamma ray, Caliper, Resistivity, PEF, Sonic, Neutron, Density) of following wells were obtained for the intended research work:

a. Miano-03
b. Miano-04
c. Miano-09

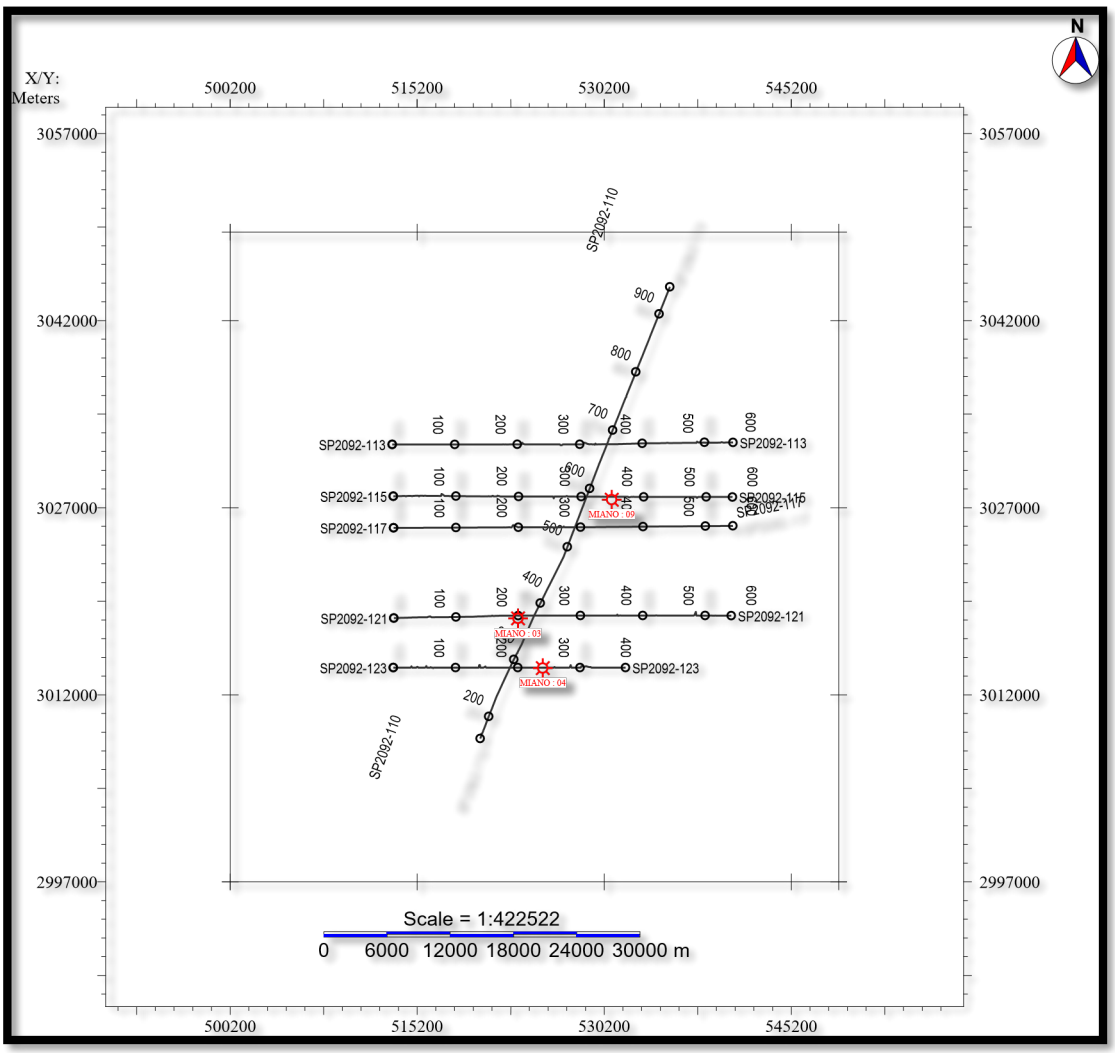

Figure 1.2. Base map of Miano Field with well locations marked.

1.8 Research methodology

To achieve the previously mentioned targets the philosophy received was to relate the seismic properties to the well properties. For this reason, using seismic attribute analysis and seismic interpretation, the Lower Goru B sands were mapped. In order to know the volume of shale, porosity, water saturation and saturation of hydrocarbon in the area of interest, petrophysical investigation of the well logs was done. The geological property namely porosity was further estimated using deterministic model based inversion. In light of the relations achieved from the petrophysical investigation, the properties gained from inversion model were identified with the values from seismic. Subsequently, sweet spots were set apart for further development of this field. The SMT Kingdom software was utilized for interpretation of structure and analysis of seismic attribute. Petrophysical analysis was carried out using LMKR Geographix and lastly, seismic inversion was completed in CGG Hampson Russel suite. The adopted research methodology is displayed in figure 1.3.

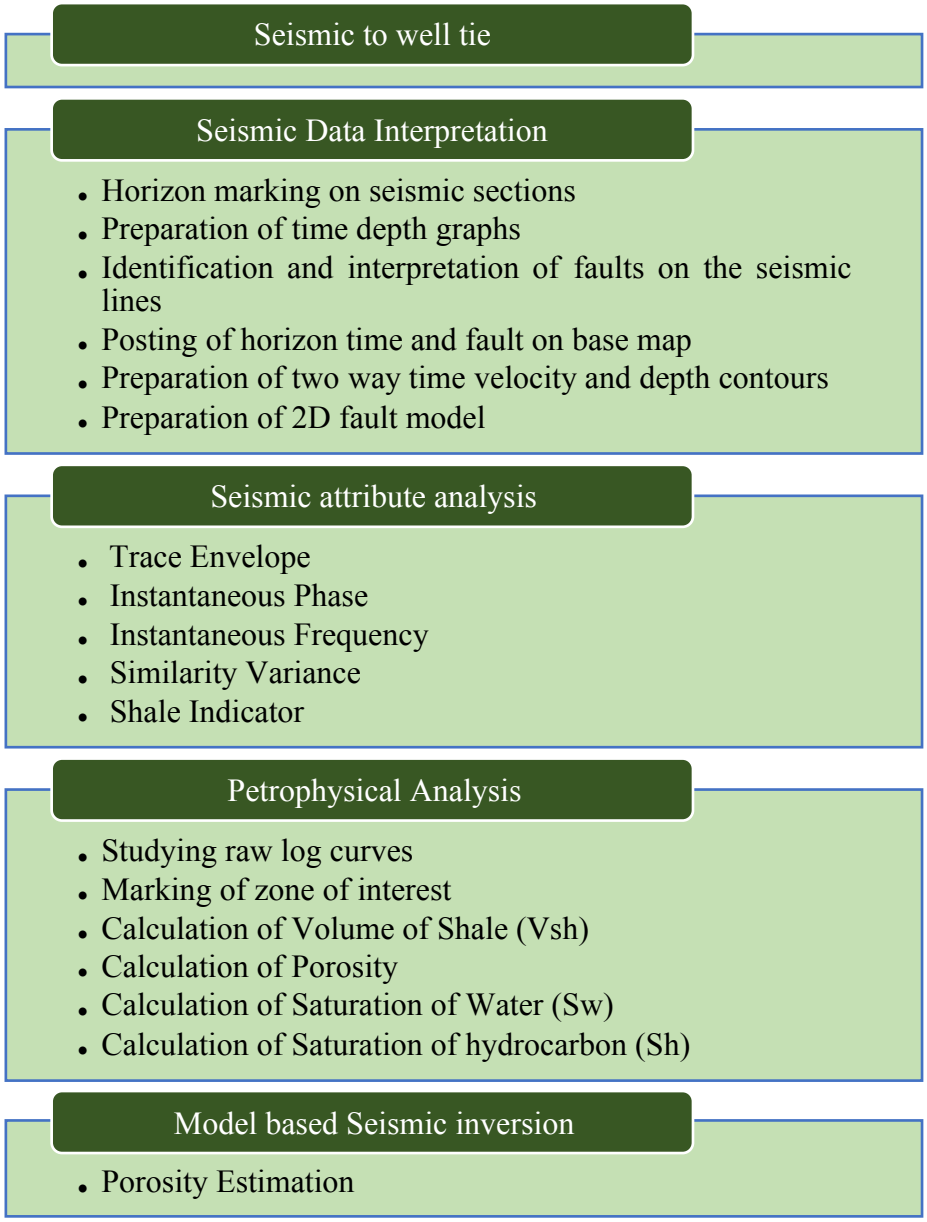

Figure 1.3. General Research Methodology

CHAPTER 2

TECTONIC AND GEOLOGICAL SETTING OF THE AREA

2.1 Regional Tectonic Setting

With respect to current regional tectonic setting, Pakistan is positioned on the North western part of the Indian Plate (Kemal, 1991) and comprises two main basins namely Indus Basin and Balochistan Basin that covers majority of its entire area. Indus Basin occupies the western edge of the Indian plate margin, it spreads to east and southeastward into India and westward into Balochistan Basin and continues northward into Afghanistan and westward into Iran. Pakistan's sedimentary basins acquired their form during Cenozoic (65 Ma-Present. Development of Indus Basin is attributed to the impact of the subducting Indian plate with the overriding Eurasian plate in the late Eocene (Ahmed and Ahmad, 1994) and possibly tectonic events linked to plate movements (Late Paleozoic-Recent) resulted in primary structural and stratigraphic features (Wandrey et al, 2004). In contrast, the formation of Balochistan was a result of subduction of Arabian oceanic plate beneath Afghan-Lut block of the Eurasian plate. Afghanistan and westward into Iran. Pakistan's sedimentary basins acquired their form during Cenozoic (65 Ma-Present. Development of Indus Basin is attributed to the impact of the subducting Indian plate with the overriding Eurasian plate in the late Eocene (Ahmed and Ahmad, 1994) and possibly tectonic events linked to plate movements (Late Paleozoic-Recent) resulted in primary structural and stratigraphic features (Wandrey et al, 2004). In contrast, the formation of Balochistan was a result of subduction of Arabian oceanic plate beneath Afghan-Lut block of the Eurasian plate.

Figure 2.1 represents sedimentary basins of Pakistan and their boundaries, MBT bounds Indus Basin from north, from east by Indian shield, western boundary is marked by Ophiolite belt and to the south by offshore Indus. The boundary between Indus Basin and Balochistan Basin is marked by Bela-Muslimbagh-Waziristan Ophiolitic Belt. Indus Basin split into three sub basins frequently quoted as Upper Indus, Central Indus and Southern Indus Basin (Iqbal et al., 2014) as an aftermath of plate convergence. Sargodha High divides Upper and Central (Middle) Indus Basins whereas Middle and Southern (Lower) Indus Basins are parted by Jaccobabad and Mari Khandkot Highs (Qadri, 1995). Upper Indus Basin is further sub divided into Potwar and Kohat sub basins, Middle Indus Basin includes Punjab Platform, Sulaiman Foredeep, Sulaiman fold and thrust belt, while Lower Indus Basin entails Thar Platform, Kirthar Foredeep and Kirthar Foldbelt. (Qadri, 1995). Study area is situated in the Central Indus Basin and is constrained by Mari Kandhkot high form north, Indian Shield from east, Axial belt from west and Jacobabad-Khairpur high form south.

Regional arches i.e. Sargodha and Jaccobabad highs were reactivated due to diagonal collision of the Indian Plate with micro plates (Afghan and Iran micro Plates) and also brought about development of wrench faulting and the creation of Sulaiman and Kirthar Fold Belt (Kemal et al., 1992). Two major highs (i) Mari Khand-Khot High came to existence by tensional tectonics around Late Cretaceous in response to separation of Indo-Pak plate from Madagascar. (ii) Jaccobabad-Khaipur arch (NW-SE trending) is detached from Mari Khandkot arch by Pano-Aqil Graben (Kemal et al., 1992).

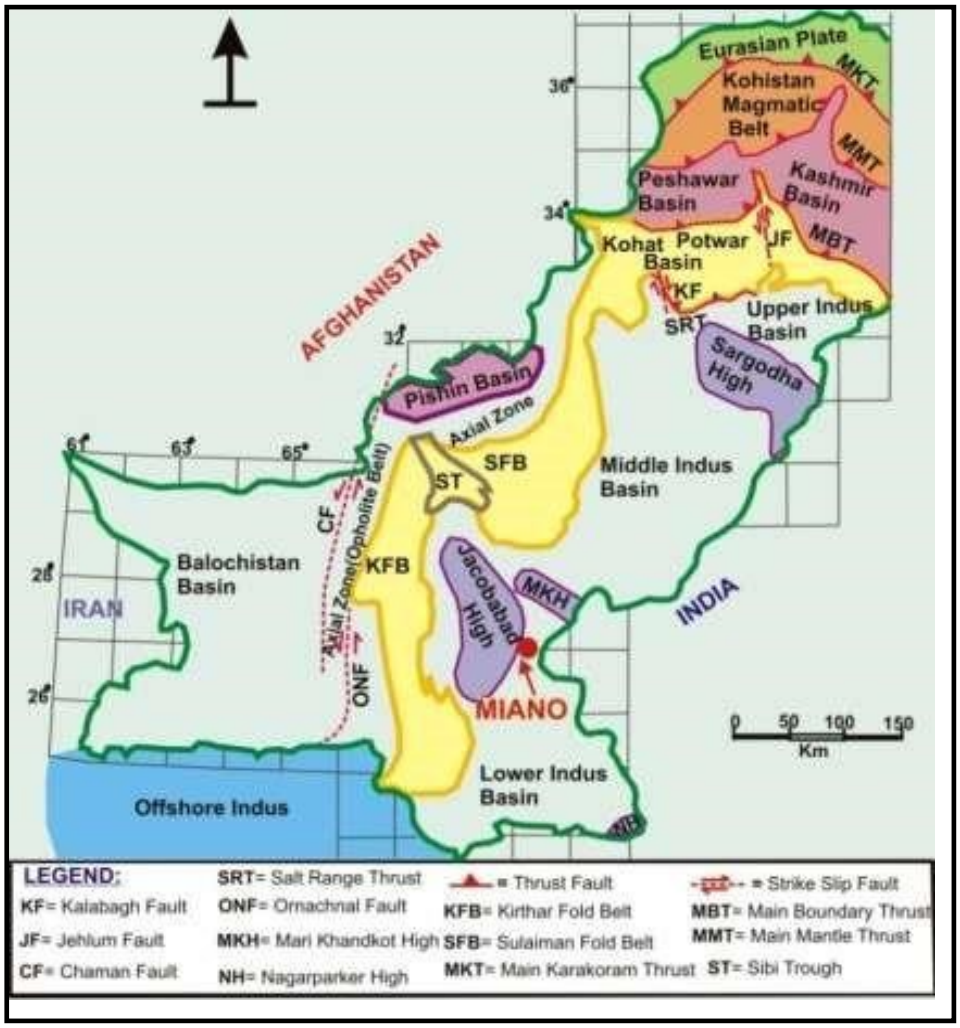

Figure 2.1. Regional tectonic setting of Miano field (Kemal, 1991).

2.2 Tectonic setting of study area

Indian plate acted like passive rift margin and on the north-western edge of it, Central Indus basin came into existence, all this was amid the age of late Jurassic to early Cretaceous. The available body of facts suggest existence of a period of 34 million years between Sembar Formation and Lower Goru (A interval). Indus Basin's closing was marked by Ghazij shale deposition (Khan et al., 2013). The first ever uplifting episode of Central Indus basin occurred near K-T boundary and this episode was marked as a tertiary unconformity. Next

uplifting episode in Central Indus basin took place amid the time of late Eocene-Oligocene and in the very same time secondary hydrocarbon relocation along with the last change to the states of traps and charge of reservoir occurred (Ahmed et al., 2012).

Sargodha high separates the Upper and Lower Indus basin. Sargodha high possesses the north of Central Indus basin. Indian shield encompasses the east. Fold and faulted belts of Sulaiman and Kirthar ranges surround the west of Central Indus basin along with Sukkur rift in south of Central Indus basin.

The study area is situated in the Central Indus Basin and is constrained by Mari Kandhkot high form north, Indian Shield from east, Axial belt from west and Jacobabad-Khairpur high form south. From the tectonic perspective, the block itself lies over panno-aqil graben which is between the two highs, famously named as JacobabadKhairpur and Mari-Kandhkot. It has Thar Desert at its south and Delhi Aravalli at its east. Study area is regionally heterogeneous fluvial-deltaic depositional environments consisting of channels sand reservoirs.

2.3 General geology of Miano area

Miano gas field is situated close to Sukkur district in Central Indus basin. Based on tectonics, Miano block lies on Panno-Aqil graben and is between KhairpurJacobabad high and Mari-Kandhkot high (Raza et al., 1990), as shown in figure. Directionally speaking, on the west of Miano field lies Karachi foredeep, Sulaiman foredeep and Sulaiman fold belt is bounded at the north of it, whereas Khairpur high lies over the eastern flank of Miano area. The prime structural low is marked by Sargarh depression in the study area, to the north-east of which lies Mari-Kandhkot high, to its south lies Thar slope, Aravalli range is to its east, and north-west has KhairpurJacobabad high. Structural as well as stratigraphic traps grace this gas prone area. As it is known that area underwent drifting preceded by rifting, caused the transtensional activity in the

formations of Cretaceous age influencing a negative flower structure in the area under study (Jadoon et al., 2015).

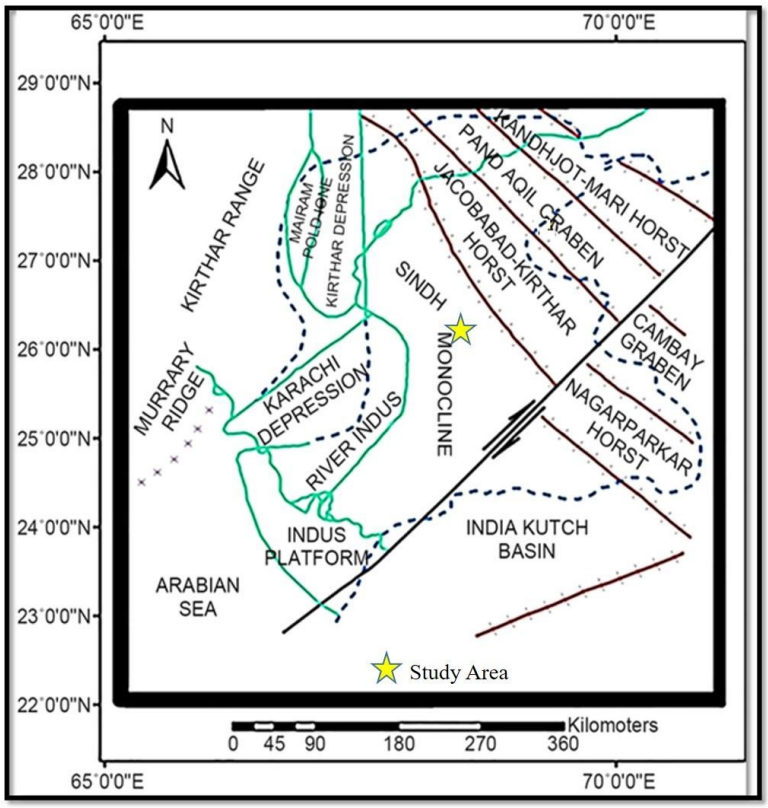

Figure 2.2. Geological setting of Miano area. The location of study area is highlighted with yellow star (Krois et al., 1998)

2.4 Generalized stratigraphy of Central Indus basin

The summed-up stratigraphy of Central Indus basin ranges from a formation belonging to Triassic age namely Wulgai to a formation of Pleistocene age name Siwaliks. The upper Triassic is by far the oldest stratigraphic unit drilled in Central Indus basin. Different erosional times of variable lengths are available. There exists an unconformity between the Goru formation (lower most Cretaceous sediments) and Carbonates of Jurassic age (Qadri, 1995). The westward prograding Sembar Formation towards basin is progressively younger and ages as it progresses towards the east as displayed in figure 2.3.

	BASIN		CENTRAL INDUS BASIN	OBJECTIVES
Era	Age	Epoch	Formation	
CENOZIOC	Quaternary	Pleistocene	Siwaliks	
	Tertiary	Pliocene		
		Miocene		
		Oligocene		
		Eocene	Pirkoh	
			Habib Rahi Limestone	
			Ghazij	
			Sui Main Limestone	
		Pleocene	Dunghan	
			Ranikot	
			Khadro	
	Cretaceous	Late	Pab	
			Mughal Kot	

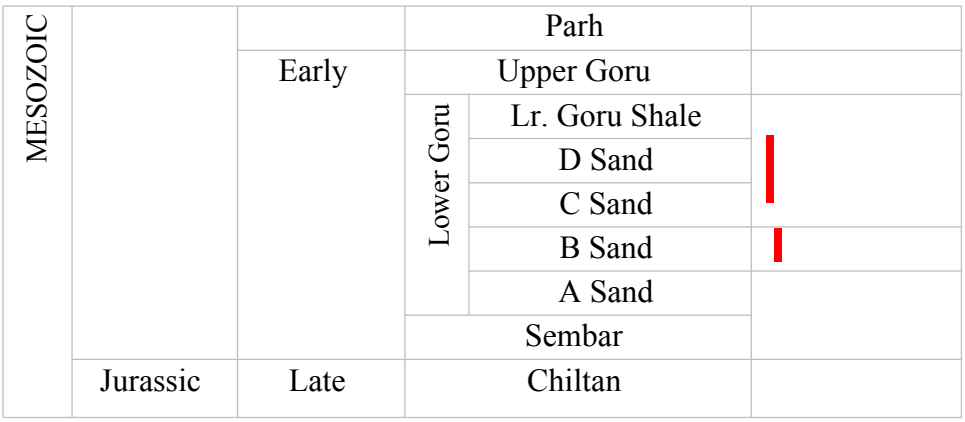

Figure 2.3. Generalized Stratigraphy of the Central Indus Basin, with study objectives highlighted with red color (Krois et al., 1998)

2.5 Stratigraphy of Study area

Based on drilling data from Central Indus Basin, sedimentary sequence ranges from Jurassic to Recent as outlined in figure 2.3. It is essentially a natural gas bearing zone and contains some of the largest discovered gas fields in Pakistan (Sui Gas field with 8.6 TCF recoverable reserves), other noticeable names include Qadirpur, Uch, Zin, Loti etc, Main producing horizons range in age from Cretaceous (Lower Goru sands and Pab sandstone) to Eocene (Sui Main Limestone, Habib Rahi Limestone and Pirkoh Limestone). Figure 2.3 outlines the stratigraphic column of Central Indus Basin and the relevant formations of the study area (Miano-03, Miano-04 and Miano-09) are described in proceeding section.

2.5.1 Cretaceous stratigraphy

The Cretaceous period was the time of structural flimsiness and amid this period numerous new features came into existence including the Lasbela and

Central anticlines and also resulted in the separation of Baluchistan Basin into (two) sedimentary sub basins (Shah, 2009). Detachment of Eastern and Western Gondwanaland additionally happened in Early Cretaceous. The formations namely Sembar and Goru demonstrate the division of India from Eastern Gondwana around 120 million years prior (Qadri, 1995).

2.5.1.1 Sembar Formation

The formation of Sembar consists of dark shale, which is interbedded with siltstone, argillaceous and nodular limestone. Glauconitic silt is normally observed. On the upper side, Sembar Formation has a contact with Goru formation which is gradational and an unconformable lower contact with Jurassic formations (Kazmi and Jan, 1997).

2.5.1.2 Goru Formation

Goru formation's lithology consists of calcareous shale and sandstone. In light of the lithological variance, it is split into Upper Goru formation (upper shale unit) and Lower Goru formation (sandy part) (Qadri, 1995). Exploration and production companies additionally have particular codification for Lower Goru formation.

2.5.1.3 Lower Goru Formation

Lower Goru indicates deposition in inner to outer shelf setting, in this predominantly silliciclastic formation multiple sequences can be recognized for Lower Goru Formation each of which comprises multiple genetically related

packages with multiple sandstone bodies. Alternating sandstone bodies are separated above and below by regionally extensive shales and the sandstones from each sequence contains one or more reservoir quality sandstone intervals (Ahmad and Khan, 2010).

2.5.1.4 A interval

The A interval of Lower Goru formation is also called as Massive sand interval. The separation of Madagascar and India from Antarctica and Africa plates completed 94 Ma amid late Cretaceous age. This separation in turn led to the formation of a basin that was marine in nature. A sand is predominantly composed of sandstone with inter bedded shale and directly overlies Sembar Formation. Both, lower contact with Sembar Formation and upper contact with Basal sand is conformable (Qadri, 1995).

2.5.1.5 B interval

Lower Goru B interval is also called as Basal sand interval. B sand represent tidal channel sandstone deposited in high energy water. This hydrocarbon producing interval is penetrated by study wells and represents deposition in overall transgressive environment. Compositionally it is made up of alternating sequences of sand and shale and the shale in this interval is thought to act as a seal. The shale here may behave as a lateral and bottom seal (Qadri, 1995).

2.5.1.6 C interval

C sand of Lower Goru Formation is also known as Middle Sand and composed chiefly of sandstone with inter bedded shale. The interbedded shales

are believed to act as a top seal. C sand reservoir quality is also being investigated vigorously in Miano field as a secondary play (Qadri, 1995).

2.5.1.7 D interval

The term Upper sand interval is often used for Lower Goru D interval. Stratigraphically, the D interval of Lower Goru formation contains shale intercalations and sandstone. Upper Sand is the formal nomenclature used by other E&P companies for Lower Goru D sand. Again this interval sandstones being the dominant (Qadri, 1995).

2.5.1.8 Lower Goru Shale Interval

Directly in contact with Upper Goru Formation is the Shale unit of Lower Goru Formation which is dominantly composed shale with some minor beds of sandstone. The thick Lower Goru shale unit acts as a regional seal (Qadri, 1995).

2.5.1.9 Upper Goru Formation

The Upper Goru formation consists of shale. Additionally marl with small beds of limestone exists, demonstrating depositional environment being deep water and is going about as a seal for the Lower Goru formation's sandstone reservoir (Ebdon et al., 2004). The Goru formation is overlain transitionally by Parh formation belonging to Cretaceous age.

2.5.2 Tertiary stratigraphy

Amid the tertiary time, the confluence of Indian and Eurasian plate resulted in formation of numerous uplifts in the zones of southern Indus basin (Qadri, 1995). The Ranikot formation itself is split into three members namely, Khadro member, Lakhra member and Bara member. Shale, sandstone having interbedded limestones belong to Khadro member, shale, limestone and sandstone are seen in Lakhra Formation whereas Bara Formation contains sandstone and shale. Laki formation which is of Eocene age lies above Ranikot Formation (Kazmi and Jan, 1997).

2.5.2.1 Parh Limestone

Open marine shelf carbonates of Parh Formation is approximately 150 meters thick in the sub surface as confirmed by drilled well data. This open marine shelf carbonate Formation was deposited during Late Cretaceous age (Wandrey et al., 2004) and is predominantly composed of Limestone. Parh formation has conformable lower contact with Upper Goru Formation while upper contact with Ranikot Formation is disconformable (Shah, 1977).

2.5.2.2 Ranikot Formation

Carbonates of Cretaceous age represented by Parh Formation give way to unconformably overlying clastics of Ranikot formation (Paleocene) and is confirmed by well data from the study area. Compositionally the formation is made up of fluvial sandstones along with intercalation of estuarine shale, representing Paleocene age Lowstand system tract (Wandrey et al., 2004). Both contacts, upper contact with Sui Main Limestone and lower contact with Parh formation is unconformable (Shah, 1977). Ranikot Formation is divided into Upper and Lower Ranikot with Lower Ranikot being sandstone reservoir and upper Ranikot predominantly made up of shale.

The Lower Ranikot Formation has been documented as reservoirs in the Suliaman and Kirthar ranges, however no hydrocarbon shows in in Miano field have been recorded.

2.5.2.3 Sui Main Limestone

Early Eocene, backstepping shelf carbonates of Sui Main Limestone (SML) is documented in the study area with an average thickness of 200 meters and act as the most prolific hydrocarbon reservoir of the Central Indus Basin. The formation mainly contains limestone with shale intercalations and its upper contact with Ghazij Formation is conformable whereas its lower contact with Ranikot Formation is unconformable (Shah, 1977).

2.5.2.4 Ghazij Formation

Ghazij Formation consists mainly of Shale with occasional sandstone beds deposited in open marine setting and belongs to Early Eocene age. Ghazij Formation conformably overlies SML whereas upper contact with Kirthar Formation is disconformable (Shah, 1977). Ghazij shale due to its immense thickness and lateral extent is regarded as a regional seal.

2.5.2.5 Kirthar Formation

Kirthar formation represents a range of members each with its own of depositional setting starting from marine shales (Baska shake) at bottom through platform carbonates of Pirkoh Formation and finally to open marine shales of Drazinda member. Deposited during Middle to Late Eocene age, Kirthar Formation is mainly composed of Limestone, sandstone shale and marl (Kazmi and Jan, 1997).

Kirthar Formation is divided in to four distinguishable members that were encountered in study wells, which are as follows (older to younger):

1. Habib Rahi Limestone Member (HRL)
2. Sirki Member
3. Pirkoh Member
4. Drazinda Member

Kirthar Formation has unconformable contacts with both overlying Ghazij Formation and underlying Siwalik Formation (Shah, 1977).

2.5.3 Neogene and Quaternary stratigraphy

In Eocene/Oligocene epoch, the collision of Indian and Eurasian plates resulted in the formation of a new source of sediment supply, which, a short time later became the cause of the deposition of Siwalik group. Alluvium deposits overlie this group. There is no prospective for the amassing of hydrocarbons in such formations (Ahmad et al., 2018).

2.5.3.1 Siwaliks Group

Siwalik group (Chinji Formation, Nagri Formation, Dhok Pathan Formation and Soan Formation) represents the fresh water (molasse) deposits of Pliocene age and due to their immense thickness act as overburden rock and are attributed to have helped achieve thermal maturity and ultimately hydrocarbon expulsion. Siwalik Group has been encountered in the study area and its lower contact with Kirthar Formation is unconformable (Shah, 1977).

2.6 Petroleum System of Miano area

For a petroleum play with a monetary aggregation of hydrocarbons following variables are important which incorporate a reasonable source rock, legitimate maturation of the source rock, powerful migration capability, permeable reservoir rock, impermeable seal and trap. Natural enrichment, thermal development and any of the three types of kerogen in shale of the Sembar and Lower Goru formations of early cretaceous age make them productive hydrocarbon hotspot for hydrocarbons of the area.

2.6.1 Source rocks

The source rock of Central Indus Basin which is well established in this region is Sembar Formation belonging to early cretaceous age. Thriving source rocks capable of generating gas exists within Sembar Formation as they have achieved their desired level of maturity.

The overall ascend of ocean level which thus influenced the organic life to prosper was due to the beginning of Cretaceous. Besides, basin with anoxia caused the safeguarding and subsequent preservation of the organic matter. The organic matter which successfully got preserved transformed into hydrocarbon as a result of both pressure and temperature being under favorable conditions. All through lower to middle Cretaceous, Central Indus Basin has a zone of extensional tectonics connected with to some degree restricted circulation of ocean water at north western edge of Indian plate. When basin was opening and anoxia was setting up, the lower Cretaceous source rocks were then deposited. Similarly, clastics got deposited amid middle to upper cretaceous under favorable conditions.

Lower Cretaceous Sembar Formation is responsible for the bulk of hydrocarbons being produced in the Indus Basin. Various geochemical analysis was made on rock samples, Lower Cretaceous Sembar Formation in Indus basin which proved it as a thriving source rock. Shale is the primary source rock of Sembar formation which were deposited in shallow marine environments, having type-II and type-III kerogen containing total organic carbon content (TOC) going from under 0.5 percent to in excess of 3.5 percent, however on average the TOC of Sembar is roughly 1.4 percent. Values of Vitrinite reflectance (R_o) range from immature (< 0.6 percent R_o) to over mature (>1.35 percent R_o). Amid Paleocene and Oligocene started the thermal generation of hydrocarbons around 65-40 Ma ago. Hydrocarbon ejection, relocation and entrapment are deciphered to have happened for the most part 50 to 15Ma amid Eocene to Miocene time, before and contemporaneously with the buildout of structural traps in reservoirs of Upper Cretaceous and Tertiary.

2.6.2 Reservoir rocks

Central Indus Basin comprises of thick and diverse accumulation of rocks ranging in age and composition. Reservoir rocks are represented by Cretaceous age Lower Goru Sands, Pab Sandstone, Pliocene age Lower Ranikot Formation to Eocene carbonates of Sui Main Limestone, Habib Rahi Limestone and Pirkoh Limestone. The depositional facies of the reservoir horizons particular to the study area and target reservoir is related to shoreline and estuarine sedimentation. Reservoir quality sands are developed in the high energy shoreface to foreshore facies of the prograding shoreline (Krois et.al, 1998).

2.6.3 Seal rocks

Shales mark the seals in the system. Shales are interbedded with sands and are overlying the reservoirs. Fields that are producing has thin shale beds as

effective seals having variation in the beds thickness. Other than this, the seals that maybe of some significance include seals above truncation traps that are impermeable and faults. The acting seals in Lower Indus Basin includes shales that are interbedded in Sui Main Limestone and the shales of Upper Goru Formation (Iqbal et al., 2011). Thick sequence of calcareous marl represented by Upper Goru Formation overlies Lower Goru Formation and acts as a regional top seal (Ahmad and Khan, 2010).

2.6.4 Traps

Stratigraphical traps majorly characterize the area and provide an efficient trapping system alongside normal faulted blocks and negative flower structures. The most efficient traps are formed by negative flower structures resulting in the formation of highs forming closures. However, extension in the area results in the formation of horst and graben structures (Ahmad and Khan, 2010).

CHAPTER 3

SEISMIC DATA INTERPRETATION

3.1 Introduction

The seismic reflection is geologically meaningful for, it marks the boundary of acoustic impedance contrast. In order to understand seismic data, it needs to be expressed in terms of geology, also the seismic data's interpretation results in depicting it in geological terms. At the point when capably did, it requires the mix of all conspicuous topographical and geophysical laws into an incorporated exhibition that will be more total and more tried and true then either the source will most likely give alone. The principle motivation driving seismic data interpretation is to get as clear a picture of the subsurface as possible (Watters, 2008). The principle goal of seismic interpretation may differ for different companies based on their focus of study, as a result it is hard to make some unequivocal standards about how one should get to their goal. However in ideal cases where we can determine interval velocity to quite a precision, lithology identification can be performed. Likewise, stratigraphic and structural analyses are two fundamental methodologies of interpreting seismic data.

3.2 Structural analysis

It is the study of reflectors geometry on the basis of reflection times. Structural analysis of seismic data is carried out to identify the structural traps in any area which are the suitable sites for hydrocarbon accumulation. Most of structural interpretation was carried out on sections having two way reflection travel time (TWT). The structural maps were created to present the geometry of the chosen reflection events by creating two way time contours of reflection times (Dobrin and Savit, 1988).

3.3 Seismic Data Acquisition

In 1992, OMV Pakistan appointed a French company CGG Veritas for 2-D seismic data acquisition in Miano field. 60-fold is the nominal fold of data with S.S.L as the crew having seismic party number 115. The format used for data acquisition was SEG-D 6250 BPI format with record length of 5sec and 2ms being the sampling interval along with total traces 120. The seismic data used for this research was PAM- preserved amplitude mode migrated data.

Table 3.1. Source and geophone parameters used during seismic data acquisition

Source parameters		**Geophones parameters**	
Vibrator	FAILING Y2700	Geophone type	SM4 UB 10Hz
Pattern	4 units in line	Geophones per group	36
Vibrator spacing	15m	Geophone interval	4.16m
Number of sweeps per vibrator	8	Group distance	50m
Sweep	10-64Hz (10sec)	String spacing	3m
V.P interval	50m	Array length	50m
Array length	88.75m		
Drive	85%		

3.4 Data quality

Seismic data quality is reasonably fairly good with overall signal/noise ratio varying from line to line. The reflectivity is good at the junction between clastic and carbonate Formations. However, data underneath fault planes was of poor quality and it was difficult to define proper fault planes at Cretaceous and Jurassic levels.

Five formations were picked to carry out study in this area, includes, Pirkoh, Habib Rahi, Sui main limestone, Ranikot, Upper Goru and Lower Goru B sands.

3.5 Seismic data loading

Geographix Discovery software was used for horizon and fault marking. Seismic lines were loaded into the software in the SEG-Y format and were assigned the navigation values. Wells were loaded using their LAS files. Miano-03, Miano-04 and Miano-09 wells were loaded along with the tops of formations. Using Hampson-Russel Software, synthetic seismograms were generated and furthermore helped in the marking of horizons in Geographix after exporting the synthetic seismogram from Hampson-Russel Software and importing it into Geographix.

3.6 Seismic base map generation

After the loading of the seismic data and their corresponding navigation values, a base map is generated. Seismic base map includes one strike line (OMV-P2092-110) and six dip lines (OMV-P2092-113, OMV-P2092-115, OMV-P2092-117, OMVP2092-119, OMV-P2092-121 and OMV-P2092-229) as shown in figure 1.2. QC was performed on all seismic lines by either simply viewing them and in other times by adjusting their scales for better seismic resolution which help in horizon picking, fault demarcation and structure identification.

3.7 Steps for seismic data interpretation

Keeping in mind the end goal which is interpretation, seismic data was used in SEG Y format. The data of well tops alongside seismic sections was additionally required. In the wake of marking of the reflectors, for to create the

time contour maps, the travel time of seismic waves to the reflectors and back to the geophone was noted. To get depth contour maps, time values were converted to depth. This was done using the product of velocity into time values which were determined after performing velocity analysis. Depth contour maps likewise were created using Kingdom software.

3.8 Selection of control line

For effectively picking the horizons and marking the faults on a seismic section, it is smarter to have a control line, such that the well lies on top of one of the seismic lines given. This is what is referred to as a control line using which the rest of seismic lines can be tied. In our research, the line P2092-121 is marked as the control line as the well Miano-03 lies on this line and using it the reflectors were marked for all the seismic lines as shown in figure 1.2.

3.9 Synthetic seismogram generation and reflector marking

Statistical wavelet is extracted from a seismic line to generate synthetic seismograms for well Miano-03 each, using kingdom software. The information gathered from the synthetic seismograms provides the actually points to begin marking horizons on seismic section. Prior to that however, mistie calculation was likewise done to ensure that every one of the lines are at a similar reference datum. Minor mistie was detected in 0.05msec of data. Using synthetic seismogram of well, Lower Goru Formation along with its member were marked which are D interval, C interval and B interval as shown in figure 2.4. The formation, Lower Goru is thought to possess attributes of a potential reservoir.

3.10 Marking of faults

The faults were distinctively set apart based on discontinuity in the reflectors on every one of the seven lines. Many low and high angle horst and graben structures were perceived in seismic sections under investigation.

3.11 Well to seismic tie

In order to pick horizons accurately, well to seismic tie is made, however, to achieve that, synthetic seismogram was generated utilizing density and sonic logs from Miano-03 well. The seismic wavelet which was extracted from seismic line was convolved with the reflection coefficient series to achieve synthetic seismogram in amplitude data form. It was then compared with 2-D trace seismic section which was closer to the well, the section being SP2092-121. In order to achieve an even match throughout, constant shifts were applied to the synthetic seismogram. As a result, accurate picking of seismic horizons over seismic sections along with correlation with TD chart was achieved.

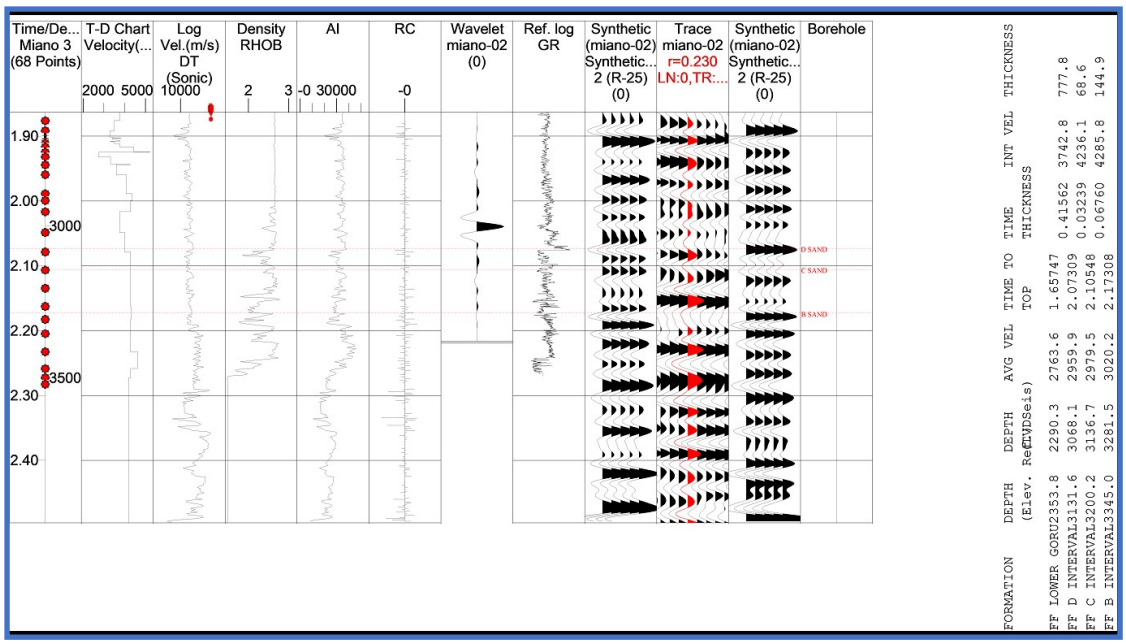

Figure 3.1. Synthetic seismogram of Miano-03 well showing horizons of interest

3.12 Horizons and faults picking

Using synthetic seismogram, four horizons were marked on the seismic line namely, SP2092-121. This was achieved by overlaying the synthetic seismogram over the seismic line. The four horizons being, top Lower Goru Formation, D interval, C interval and B interval on the seismic line were marked below well shot point. The same horizons were marked on seismic line SP2092-110 (strike line) utilizing loop tie among seismic lines.

Transtensional (extensional) regime induces normal and strike slip faults in the area. Several normal faults were marked on each dip line. No such faults were recognized on shallow horizons like Pirkoh and Habib Rahi on any seismic line. All major normal faults were penetrated down and tied with Chiltan. Some major faults were marked on all seismic lines as main faults of the area. Major disturbance is observed at the level of Lower Goru Formation and its sand members.

3.13 Seismic interpretation analysis

Seismic interpretation has indicated the presence of structural traps in Miano area. Structural analysis proves the presence of successive normal faults with horst and graben structures with tilted fault blocks present along them. Strike-slip component is also a major structural inclusion in the structure of area, causing negative flower structure in structural highs and lows of Miano area because of transtensional regime. Given Miano wells were drilled on horst structure SP2092-110 is the strike line from the available data. The orientation of this strike line is from NW to SE. Horizons were marked using synthetic seismogram. Miano-09 and Miano-03 wells were drilled near this line.

Structural high can easily be seen between 700th to 750th shot points between two faults on this seismic line as shown in figure 3.2.

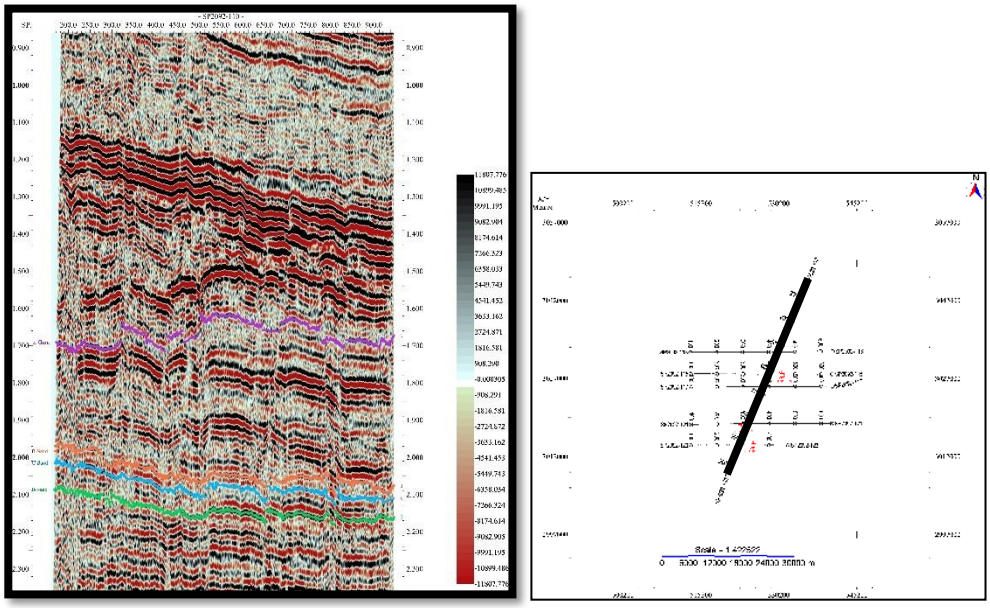

Figure 3.2. Interpreted strike line SP-2092-110.

SP2092-113 is a dip line. Control from SP2092-110 was shifted to this line via loop tie. Orientation of this line is from NW to SE. Different normal faults were marked on the basis of discontinuity and breakage in reflectors. Splays of normal faults were originated from faults with strike-slip component. Horsts, normally tilted fault blocks and grabens along with strike-slip component were the major identified structures of this seismic line as shown in figure 3.3.

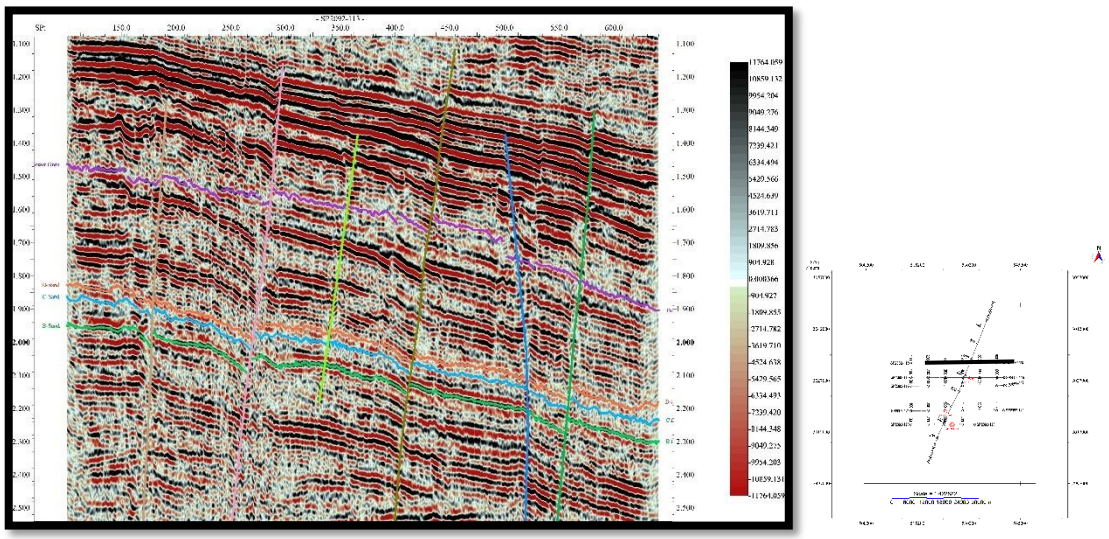

Figure 3.3. Interpreted seismic dip line SP-2092-113.

SP2092-115 suggests the dip of horizons in NW-SE orientation, while tilted fault blocks are dipping in SW direction. Many splays of faults can be seen originating from major faults as shown in figure 3.4.

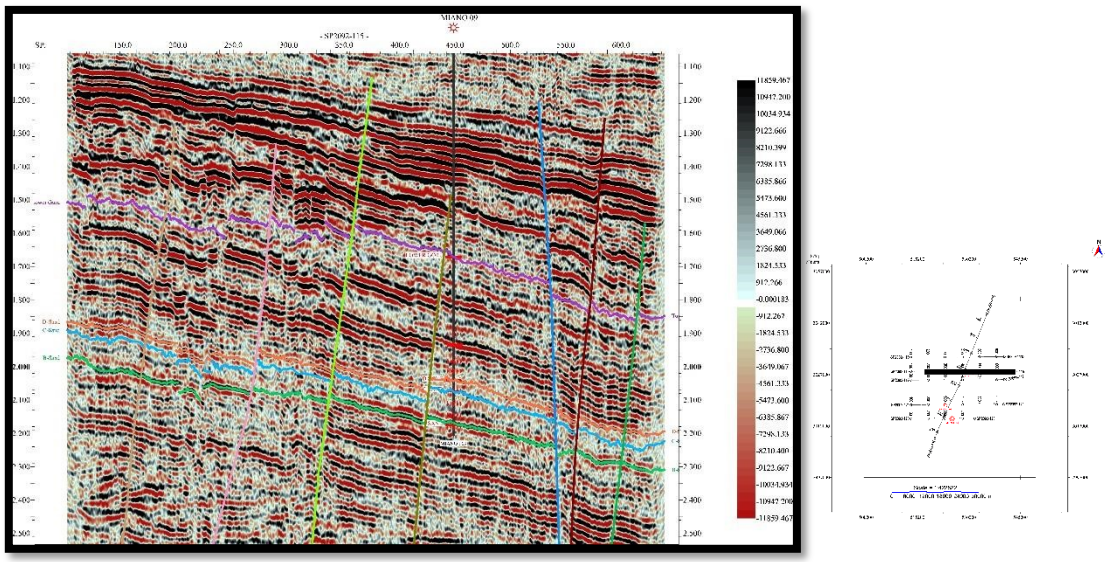

Figure 3.4. Interpreted seismic dip line SP-2092-115.

Various normal faults were marked on SP2092-117 seismic line. Five main normal faults originates from shallower level and disturbing Lower Goru Formation along with its sand members. These fault dips in SW and in SE quadrant as shown in figure 3.5.

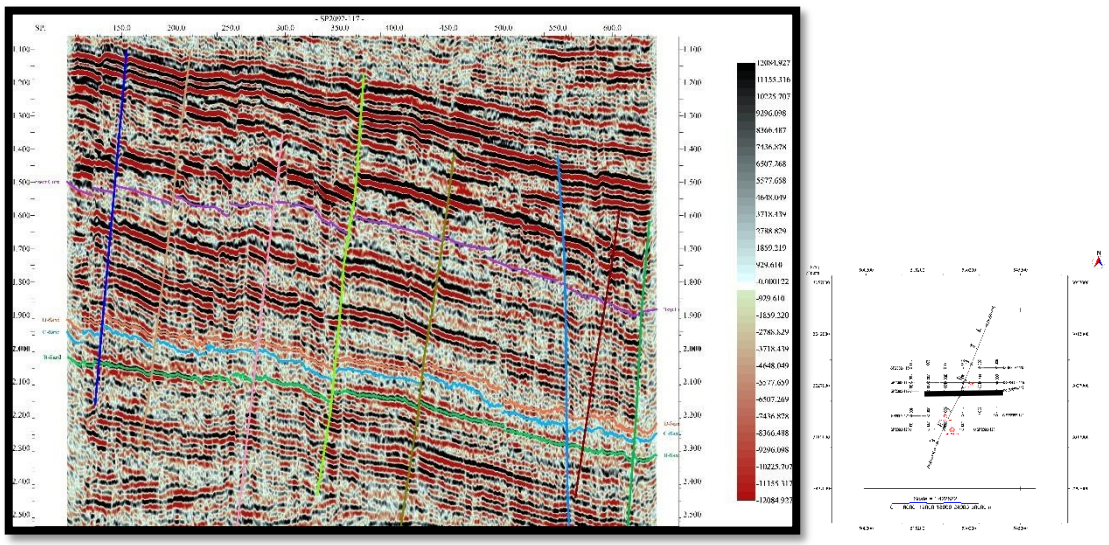

Figure 3.5. Interpreted seismic dip line SP-2092-117.

Seismic line SP2092-121 is a control line. Well Maino-03 is located on this seismic line. One major horst structure exists in the middle of this seismic line. Rest of the fault blocks are half tilted as shown in figure 3.6.

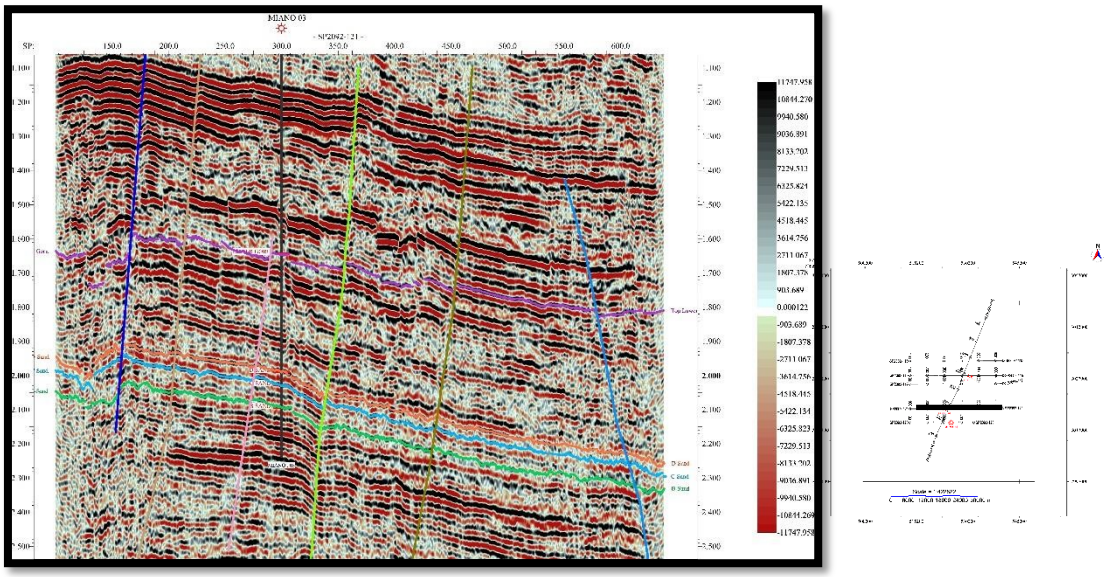

Figure 3.6. Interpreted seismic dip line SP-2092-121

3.14 Time contour mapping

After seismic structural interpretation, time grids of all horizons of interests were separately generated to extrapolate their values on entire area of seismic base map. Contours of each horizon were generated with 10 ms / 0.01 sec contour interval. Fault correlation is carried out at all horizon level to generate fault boundaries.

TWT contour map of Lower Goru Formation includes 0.015 sec contour interval with several contours got closed against faults wit. Faults are dipping in westward and eastward direction, making horst structure for Miano-03 well. The minimum contour value of Sui Main Limestone is 1.462 sec and maximum value is 1.912 sec. Structure is depicted by closure of faults in north-west and south-east orientation making a two-way dip closure for hydrocarbons to trap as shown in figure 3.7. Along with the structural support, exploration history and on field drilled wells have given the insight that Lower Goru Formation is acting as a major hydrocarbon producing formation in Miano area.

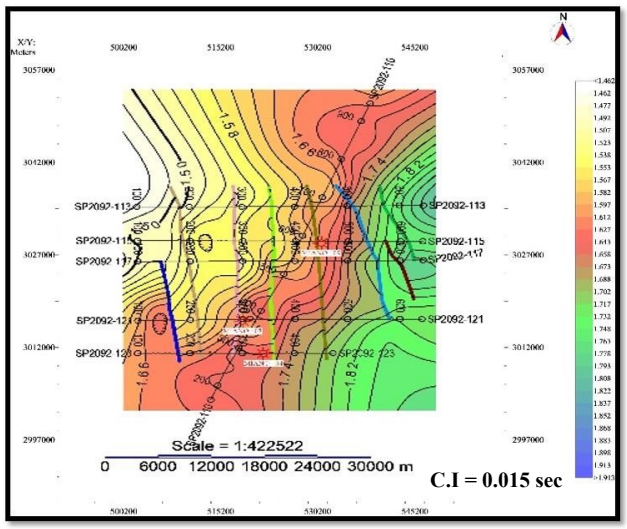

Figure 3.7. TWT contour map of Lower Goru Formation.

TWT contour map of D-Sands includes 0.025 sec contour interval and indicates formation of various closures along the fault boundaries. The minimum contour value of D-Sands is 1.830 sec and maximum value is 2.405 sec. D-Sands is shallower in the west ward direction and got deeper towards east as shown in figure 3.8.

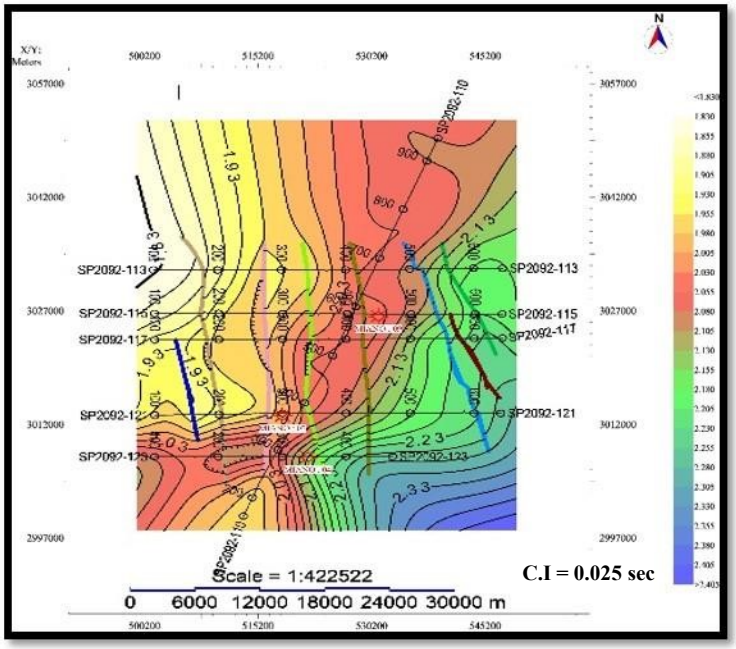

Figure 3.8. TWT contour map of D-Sands.

TWT contour map of C-Sands includes 0.025 sec contour interval and indicates formation of closures along fault boundaries. The minimum contour value of C-Sands is 1.860 sec and maximum value is 2.360 sec. C-Sands is shallower in west ward direction and got deeper towards east as shown in figure 3.9.

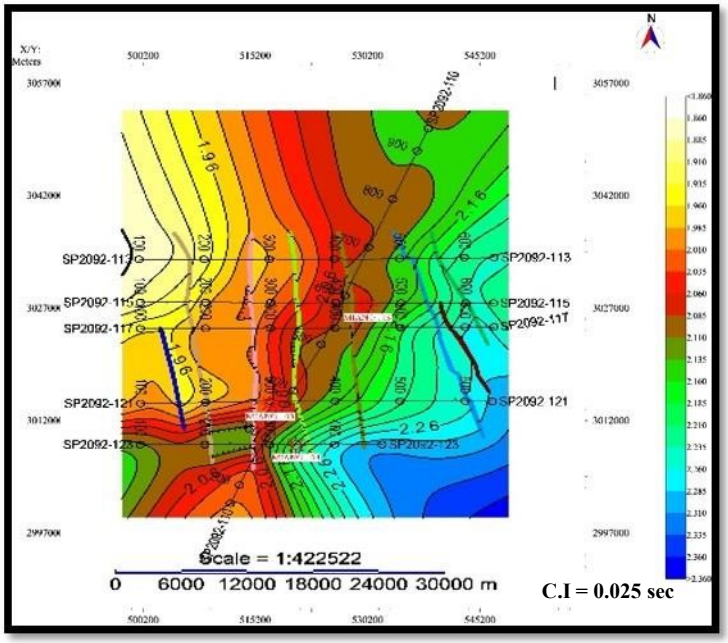

Figure 3.9. TWT contour map of C-Sands.

TWT contour map of B-Sands includes 0.02 sec contour interval with several contours got closed against faults. These faults are dipping in westward and eastward direction making horst structure for Miano-03 well. The minimum contour value of B-Sands is 1.920 sec and maximum value is 2.460 sec. Structure is enclosed by closure of faults on east and westward sides. One structural compartment is identified at north-northwest orientation against fault. This horst structure is bounded by faults from two sides and contours got closed from rest of the two sides, making a two-way dip closure for hydrocarbons to trap as shown in figure 3.10.

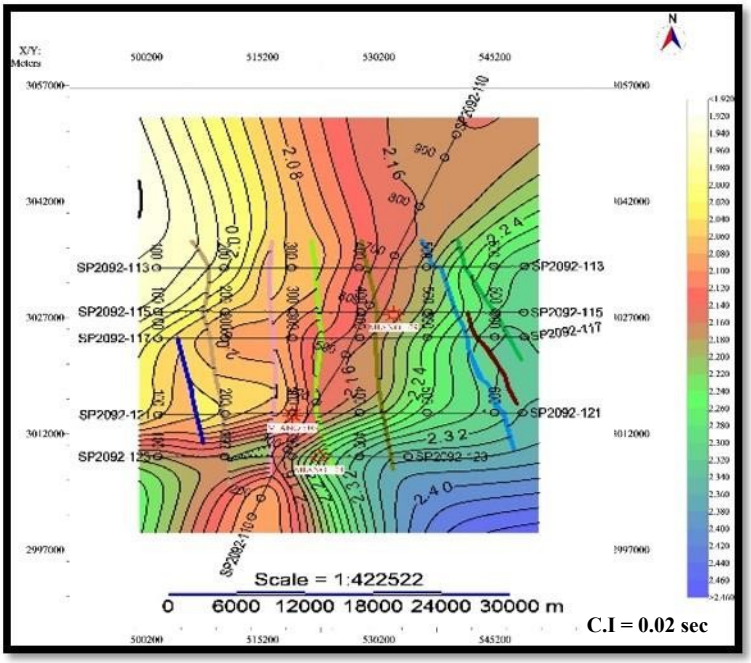

Figure 3.10. TWT contour map of B-Sands.

3.15 Depth contour maps

For depth contour mapping, firstly depth grids were made using shared TD chart. For time to depth conversion, time grids got multiplied with RMS velocity function divided by two, provide us with depth grid. In the same way depth grids for all horizons were made and depth contours were generated over it. In the depth contour maps, the orientation and dips of the structures are similar to time contour map of that formation.

Depth contour map of Lower Goru Formation uses 40 m contour interval with shallower to deeper depth trend in west to eastward direction respectively. The minimum contour value of Lower Goru Formation is 1670 m and maximum value is 2730 m. The values of depth on depth contour map at Miano-03 well is matching with the well top with reasonable accuracy as shown in figure 3.11. The contour map shows decrease in depth values at the north-northwestern compartment, making it drilling wise prospective area. This compartment is structurally bounded by horst structure which can possibly entrap hydrocarbons.

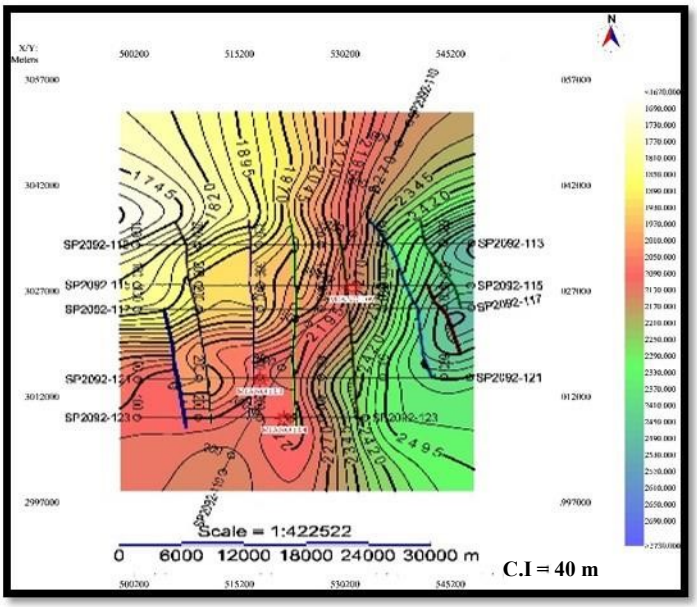

Figure 3.11. Depth contour map of Lower Goru Formation.

Depth contour map of D-Sand uses 20 m contour interval with shallower to deeper depth trend in west to eastward direction respectively. The minimum contour value of Depth at D-Sand level is 2695 m and maximum value is 3255 m as shown in figure 3.12. Depth values at Miano-03 well are matching with the well top value of D-Sand.

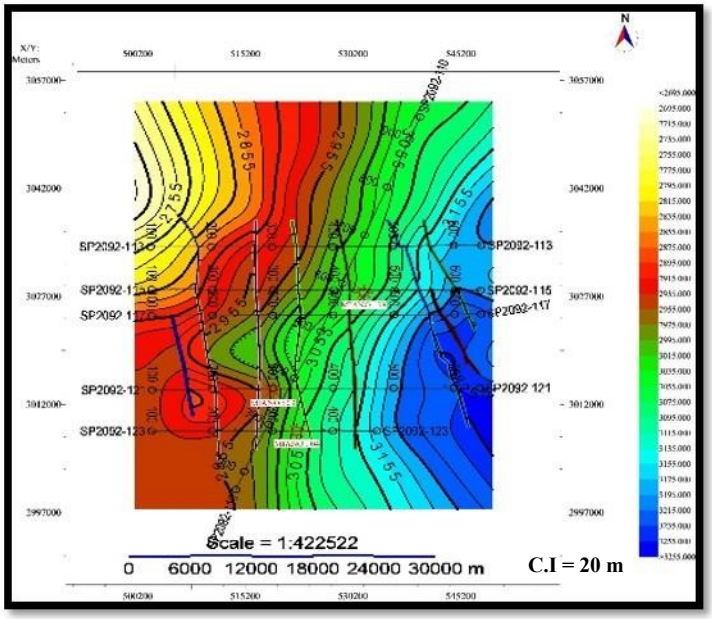

Figure 3.12. Depth contour map of D-Sand.

Depth contour map of C-Sand uses 10 m contour interval with shallower to deeper depth trend in west to eastward direction respectively. The minimum contour value of depth at C-Sand level is 2880 m and maximum value is 3300 m as shown in figure 3.13. Depth contour map at Miano-03 well location indicates that the depth of well top of C-Sand is matching with the depth computed over depth contour map.

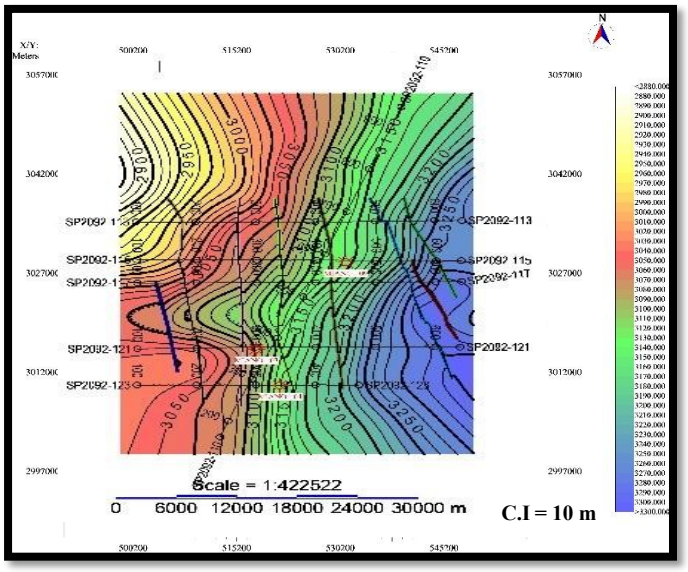

Figure 3.13. Depth contour map of C-Sand.

Depth contour map of B-Sand uses 20 m contour interval with shallower to deeper depth trend in west to eastward direction respectively. The minimum contour value of B-Sand is 3000 m and maximum value is 3500 m. Depth contour value at Miano-03 well indicates that depth is matching with the well top of B-Sand The contour map shows decrease in depth values at the north-northwestern compartment, making it drilling wise prospective area as shown in figure 3.14. This compartment is structurally bounded by horst structure which can possibly entrap hydrocarbons.

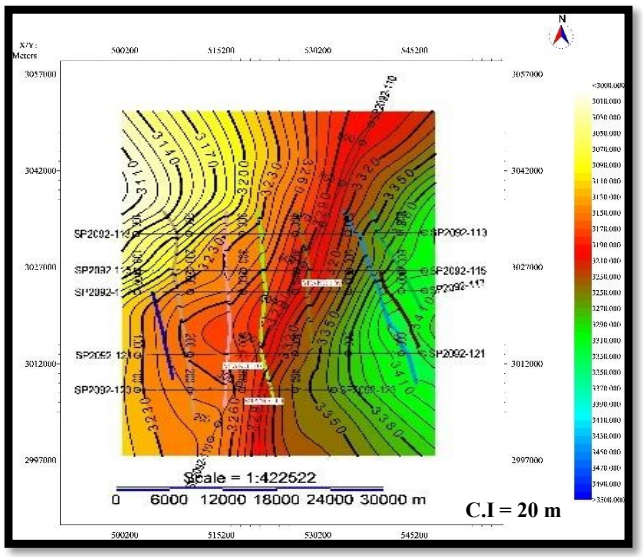

Figure 3.14. Depth contour map of B-Sand.

CHAPTER 4

SEISMIC ATTRIBUTE ANALYSIS

Seismic attributes are defined as all the implied, computed and measured quantities acquired from seismic data (Brown, 2001). Seismic attributes have been used as a tool for reservoir characterization to geoscientists and its analysis allows the structural, stratigraphic and petrophysical aspects of subsurface rocks that is beyond the resolution of and subtle for traditional seismic amplitude data. Information related to amplitude, position and shape of seismic waveform are the typical outcome of seismic attributes. Seismic attribute analysis helps interpreter in terms of fetching accurate information regarding lateral changes in horizon, stratigraphic pinchouts, continuity of reflectors, bed thickness, structural and lithological parameters of seismic prospect (Siguaw et al., 2001). Now there are more than 50 distinct seismic attributes that can be calculated from seismic data.

4.1 Classification of seismic attributes

Mainly all the seismic attributes are not independent of each other but basically they are presenting basic and limited amount of information in variety of ways. The basic seismic data information is in the form of amplitude, time, frequency, attenuation etc. and it will form the basis of our seismic attribute classification (Taner et al., 1997) as shown in in figure 4.1.

Structural information is obtained from time derived attributes while stratigraphic and reservoir information is provided by amplitude derived attributes. Additional useful information regarding stratigraphy and reservoir

along with bed thickness and microfractures identification can be derived from frequency attributes. Attenuation attributes are not yet well understood but there is a possibility that they will yield information on permeability in future. Mostly seismic attributes are derived from migrated and normally stacked data but variation in seismic amplitude or acoustic impedance contrast as a function of angle of incidence provides a further source of information. Major examples of these pre-stack attributes are AVO.

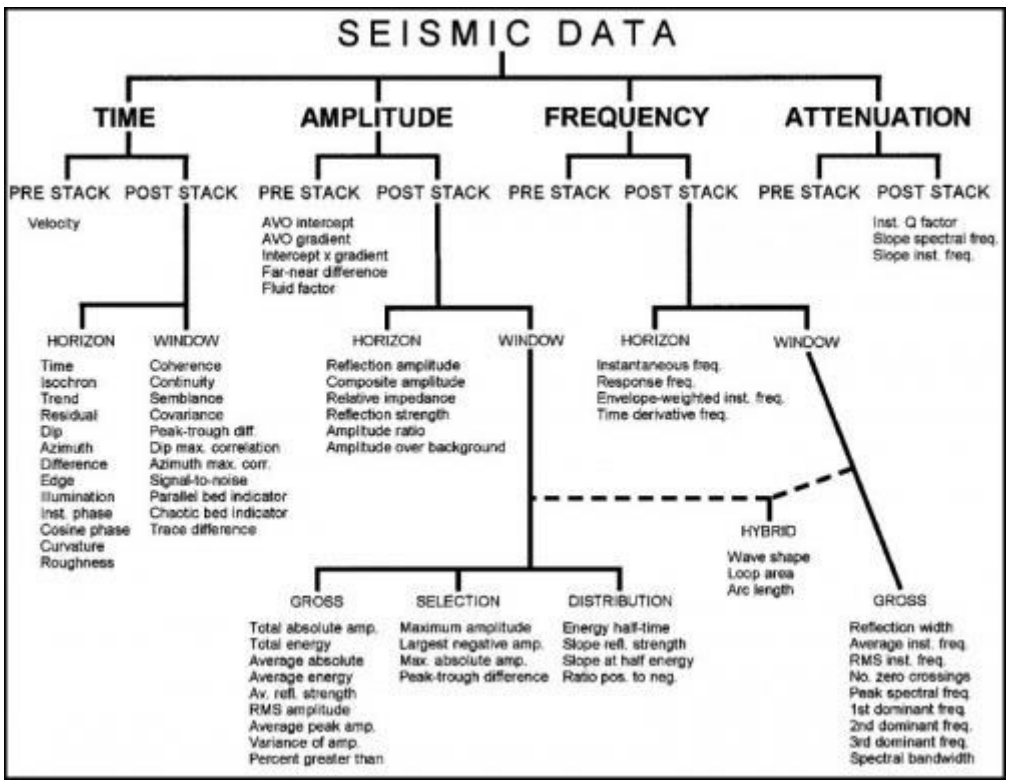

Figure 4.1. Classification of seismic attributes

Seismic attributes utilized in this research are:

a) Trace envelope (Instantaneous amplitude)

b) Instantaneous phase

c) Instantaneous frequency

d) Similarity variance

e) Shale bed indicator

4.2 Application of trace envelope or instantaneous amplitude attribute on Miano seismic lines

Trace envelope as attributes analysis strengthen amplitudes and energy of the reflector. Trace envelope was developed by Nigel Anstey in 70's for oil and gas industries, to recognize "bright spots" connected to hydrocarbon accumulations.

Trace envelop can be useful in pinpointing the subsurface discontinuities, lithological dissimilarities, changes in deposition system and sequence boundaries (Chopra et al., 2007). In Miano area the target formations includes clastic variety of rocks. The Lower Goru Formation, D, B and C sands indicates instantaneous amplitudes are comparatively low because of the presence of shale sand packages present in it. Bright spot anomaly present at the level of Lower Goru B Sands suggests the presence of hydrocarbon in Miano-03 and Miano-09 well at this level. Various lateral changes in instantaneous amplitude at particular horizon indicates the presence of different lithological units juxtaposed at that horizon. Bright spots associated with strong amplitude contrasts across lithologies and their fluid; oil, gas and water content can easily be depicted by this attribute as shown by black dotted circles on couple of seismic lines (Fig. 4.2). Therefore, caution must be taken that there is not a direct straight forward relationship between hydrocarbons and direct hydrocarbon indicators, such as bright spots, nor all bright spots should be treated as conclusive evidence of hydrocarbon accumulation but none the less for prospect generation view point, anomaly is the key (Brown, 2011).

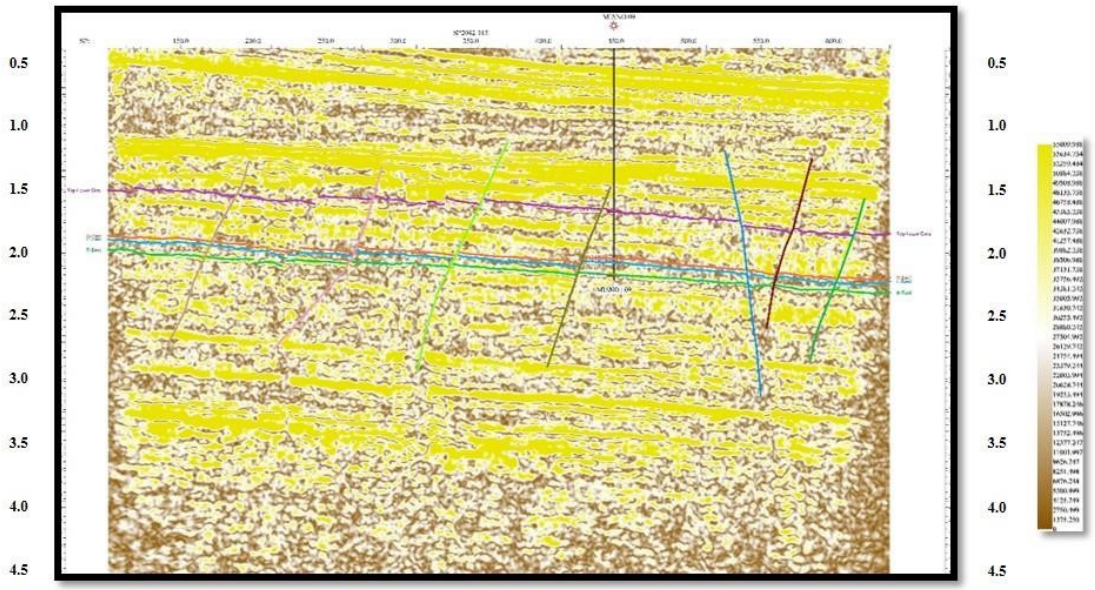

Figure 4.2. Application of Instantaneous amplitude attribute on seismic line SP2092-115

4.3 Application of instantaneous phase attribute on Miano seismic lines

The instantaneous phase relates to the position of the seismic wave front. Wave fronts are considered as lines of constant phase. The phase attribute is helpful in discriminating geometrical shape classification. It is the best indicator of lateral continuity, as shown in the figure 4.3. The high values show discontinuity while the values at Lower Goru Formation and its sand members shows a sharp continuity and are the lowest values. It gives you the best picture of sequence boundaries, seismic facies (Subrahmanyam et al., 2008).

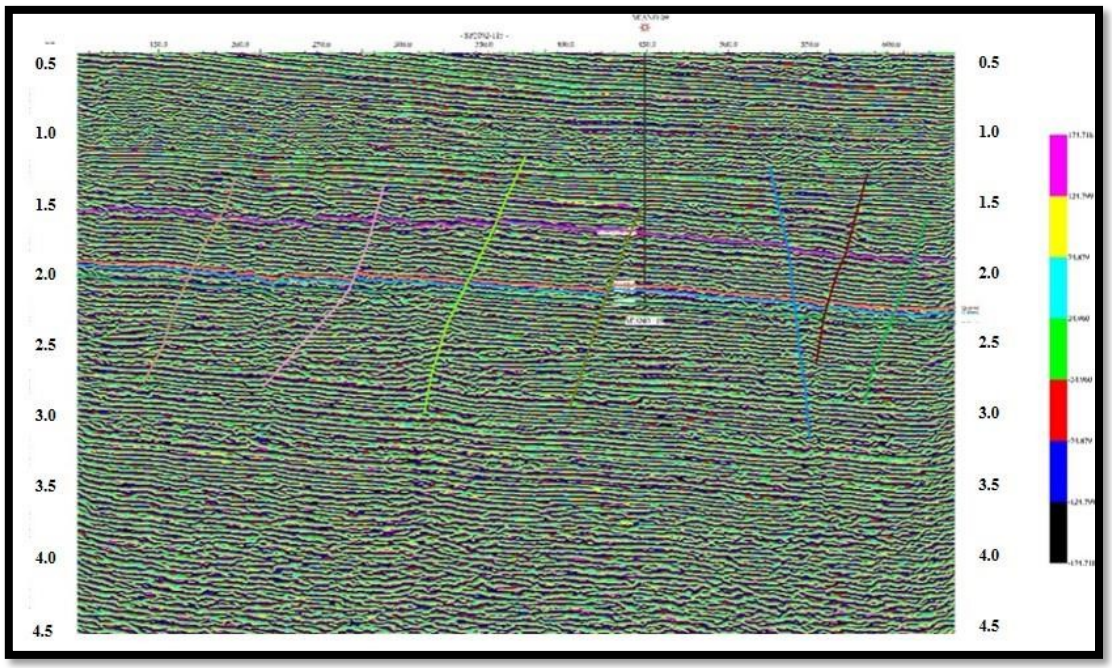

Figure 4.3. Application of Instantaneous phase attribute on seismic line SP2092-115

4.4 Application of instantaneous frequency attribute on Miano seismic lines

The instantaneous frequency (Hz) can be defined as the rate of change of phase over time. It is helpful in determining seismic features, indicator of hydrocarbons, and indicator of fracture zone. High frequencies show sharp interfaces and thin shale bedding. Lower frequencies give information about sand rich bedding. As seen in the figure 4.4 presence of high frequencies lead to presence of sand facies.

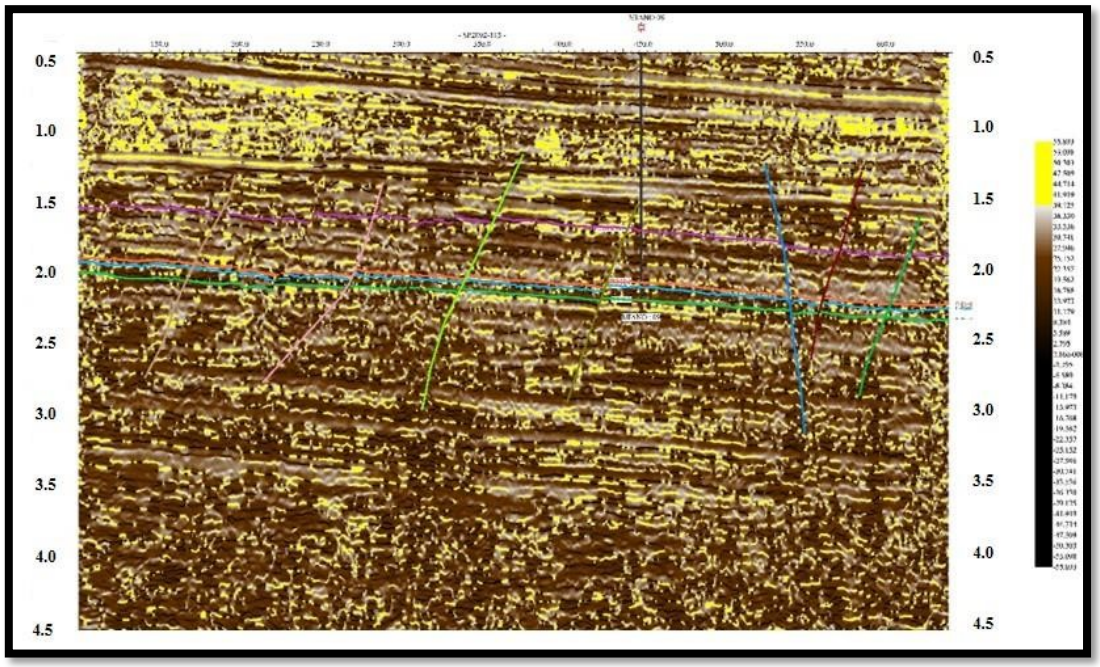

Figure 4.4. Application of Instantaneous frequency attribute on seismic line SP2092-115

4.5 Application of similarity variance attribute on Miano seismic lines

Variance attribute is an edge method. It calculates the resemblance of waveforms. Seismic attributes like frequency, bed indicator, envelope, phase, shale indicator and variance are helpful in identifying horizons. It was observed that variance displayed better response to faults than any other attribute as seen in figure 4.5.

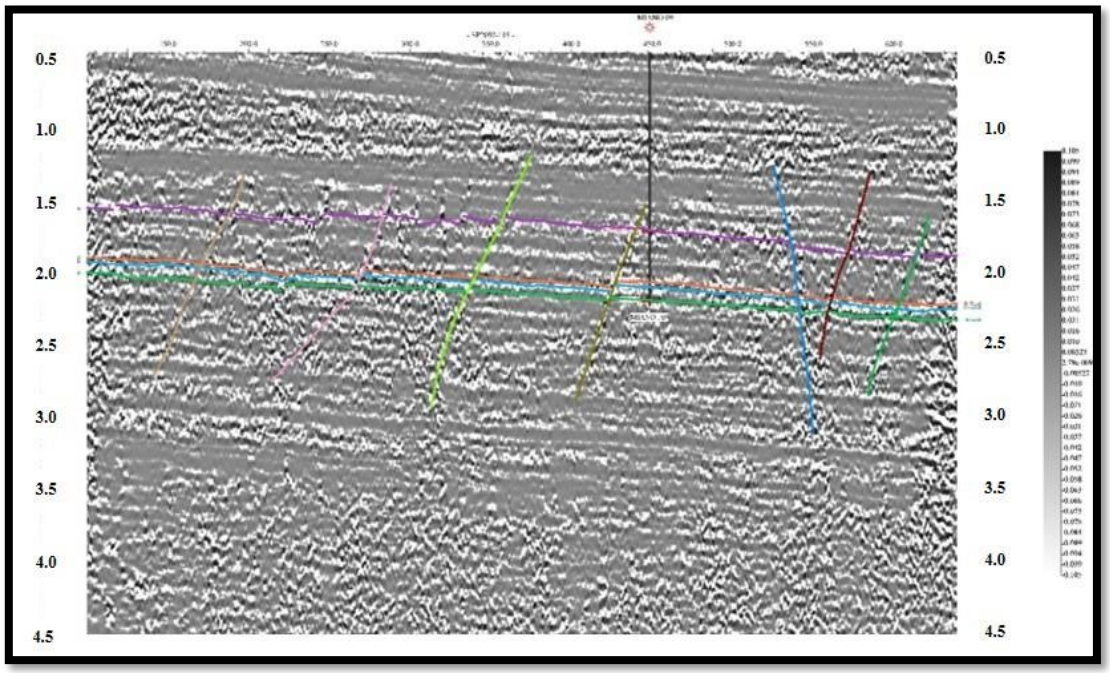

Figure 4.5. Application of variance attribute on seismic line SP2092-115

4.6 Application of shale indicator attribute on Miano seismic lines

Shale indicator is a mixed attribute. Shale beds are thin with high lateral continuity because of its depositional environment (Sampson et al., 2012). Shale indicator attribute give the information about following features:

i. High output values show the high chances of shale beds (figure 4.6)
ii. Low output values show high chances of sandstones and carbonates

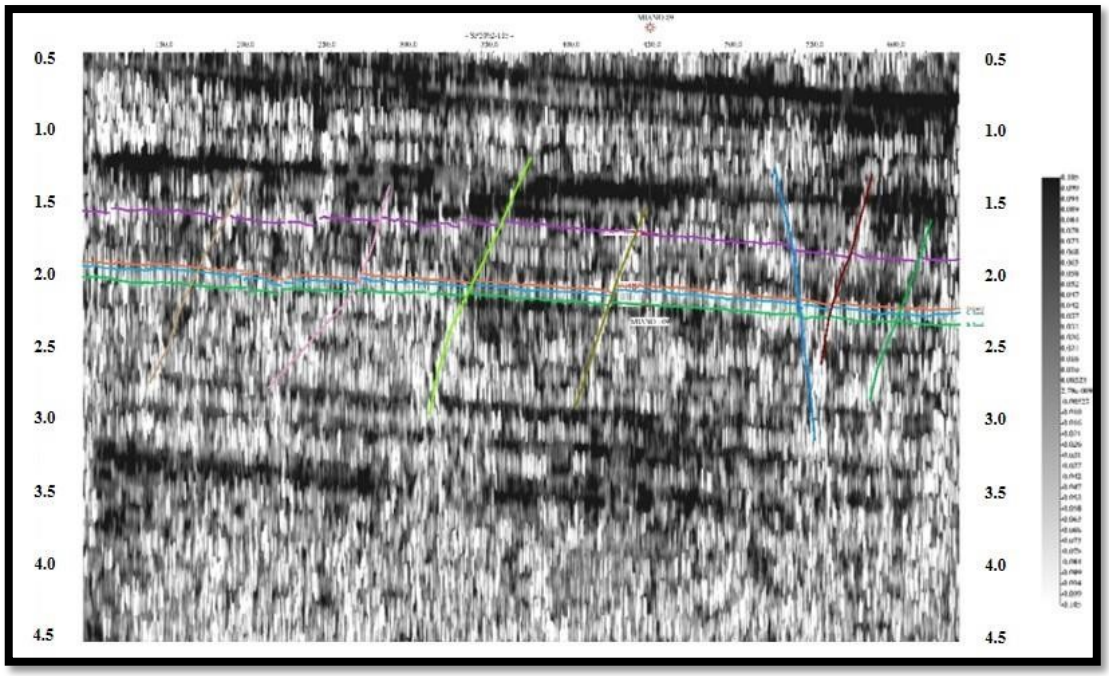

Figure 4.6. Application of shale indicator attribute on seismic line SP2092-115

CHAPTER 5

PETROPHYSICAL ANALYSIS

Petrophysics is the study of physical properties that describe the occurrence and behavior of rocks, soils and fluids. Interaction between the reservoir rock properties and fluid present in it got calculated by the help of petrophysical interpretation that allows to calculate different rock parameters like porosity, volume of shale, water saturation and hydrocarbon saturation along with the delineation of lithology, formation water resistivity, hydrocarbon presence and net pay (Petro-consultant, 1996). The complete interpretation workflow is shown in figure 5.1.

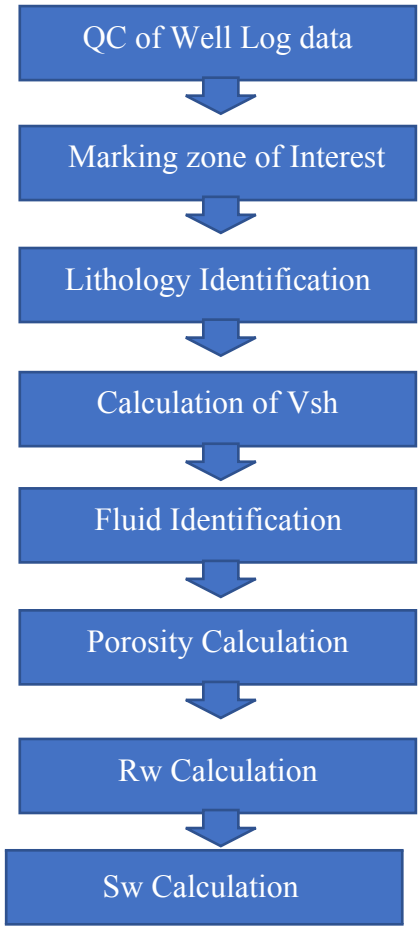

Figure 5.1. Work flow adopted for petrophysical interpretation

The first step in log interpretation is to mark the zone of interest in the raw logs. Some basic petrophysical properties like volume of shale (Vsh), porosity (φ), resistivity of water (Rw), Saturation of Water (Sw) etc. are evaluated from the well logs. This thesis covers petrophysical analysis of Lower Goru B Sands of Miano-03, Miano-04 and Miano-09 wells.

5.1 Well log data loading of available Miano wells

The raw log curves of Miano-03, Miano-04 and Miano-09 were imported in prizm that includes gamma ray (GR), spontaneous potential (SP), caliper (CALI), MSFL resistivity curve, LLS resistivity curve, LLD resistivity curve, neutron porosity (PHIN), bulk density (RHOB), sonic DT and PEF log curves. Scales of correlation, resistivity and porosity tracks got adjusted according to the

available data. GR scale lies between 0-150 API, SP ranges between -100-50 mv, caliper ranges between 6-16 inches. MSFL, LLS and LLD resistivity curves scale ranges between 0.2-2000 ohm-m. Neutron porosity scale ranges between 0.45 to -0.15 v/v, bulk density ranges between 1.952.95 gm/cc. Sonic DT log possesses a scale of 140-40 micro sec/feet where as PEF log scale ranges between 1-10 b/e.

5.2 Well log data interpretation

Different user defined equation sets are used to carry out the petrophysical analysis of well log data of Miano wells.

5.2.1 Calculation of volume of shale

Gamma ray logging is a method of measuring naturally occurring gamma radiations to determine the rock or sediments in a borehole or drill hole. It is a wireline logging method used in mining, mineral exploration, water well drilling, for formation evaluation in oil and gas well drilling and for other purposes. Different types of rock emit different amounts and different spectra of natural gamma radiations. Correlation, lithological identification and volume of shale were determined using GR log curve calculation (Petro-consultant, 2000). Volume of shale was calculated using following formula;

$$Vs = GR_{\log} - GRmin / GR_{\max} - GRmin$$

Where,

Vsh = Volume of shale (%)

GRlog = GR log reading at specific point (API unit)

GRmin = Gamma Ray minimum across interval (API unit)

GRmax = Gamma Ray maximum across interval (API unit)

5.2.2 Calculation of density porosity

Bulk density log is used for the calculation of density porosity using the following relation (Schlumberger, 2000);

$$\varnothing den = \varrho ma - \varrho b \,/\, \varrho ma - \varrho f$$

where:

φ den = Density derived porosity ϱma = Matrix density

ϱb = Formation bulk density

ϱf = Fluid density

5.2.3 Calculation of average neutron density porosity

The combination of density and neutron logs provides a good information about the porosity data, especially in formations of complex lithology. Better estimates of porosity are possible with the combination than using either tool or sonic separately because interference about lithology and fluid contents can be made. Neutron log gives us the values of porosity of rocks known as neutron porosity. Weighted average of neutron and density porosity is known as average neutron-density porosity (Schlumberger, 2000) calculated as follows;

$$\varnothing avg = Dp\ \ i + Np\ \ i2$$

where:

$\varnothing avg$ = Average porosity

$Dp\ \ i$ = Density porosity

$Np\ \ i$ = Neutron porosity

5.2.4 Calculation of effective porosity

Interconnected pores basically defines the interconnected porosity known as effective porosity, calculated as follows;

$$\varnothing eff = \varnothing avg * (1 - \text{Vshl})$$

where:

$\varnothing eff$ = Effective porosity

$\varnothing avg$= Average porosity

Vshl= Volume of shale

5.2.5 Resistivity of water (Rw)

Resistivity of water (Rw) was determined by spontaneous potential (SP) method using Sp log data of Miano-03 well. Moreover, neither of the study wells encountered any water bearing zones from which Rw value using apparent resistivity of water (Rwa) or Pickett plot method could be estimated.

5.2.5.1 SP method

The most common method to estimate Rw value utilizes spontaneous potential log, the procedure adopted is described below

<u>Step 1 Temperature gradient</u>

Using log header information the formation temperature gradient has been calculated by using following equation

Formation Temperature = (Bottom Hole Temperature * Formation Depth)/TVD

Formation Temperature = (146.1°C * 3505 m)/ 3550 m

Formation Temperature = 142.16 °C

Step 2 Static Spontaneous Potential (SSP)

Static Spontaneous Potential (SSP) is the maximum deflection of SP curve from Shale Baseline against thick clean reservoir. The shale baseline has been marked against thick shale interval (3455 m). Similarly, sand baseline has been marked against thick clean interval where SP deflection is maximum. As the Sp log is scaled -160 (left) to 40 (right) so, on ten scale division each division is equal to 40 mv. As the separation between Shale baseline and Sand baseline is 1/2 divisions therefore SSP value is +19 mv.

The Sp log signature quite clearly indicates that the formation fluid is of lower salinity than mud in the borehole (positive deflection). Hence the computed Rw from SP log will be overestimated. Resulting in higher water saturation values.

Step 3 Converting Rmf to Formation temperature

Rmf at Formation temperature is calculated by using **Gen-6 chart**. As Rmf at ~23 ^{0}C (74 ^{0}F) is > 0.1 ohm.m therefore Rmf is corrected to formation temperature by Rmfeq=0.85*Rmf.

Step 4 Calculating Rweq

Using **chart SP-1**, plot SSP (+19 mV) on X-axis draw a vertical line up to the point where it intersects formation temperature line (142 °C) now from this point draw a horizontal line at this point an oblique line is drawn which cuts the Rmfeq line and finally ends up at Rweq vertical line.

Step 5 Calculating Rw

Using Chart **SP-2** calculate Rw by plotting Rweq against formation temperature. Entering the Y-axis by plotting Rweq value and extending it to the temperature line. At the point of intersection draw a vertical line downwards onto the X-axis, the intersection point marks the Rw value.

Table below summarizes the Rw calculation and related variables involved in its calculation. Static spontaneous potential (SPP) is the deflection of SP against a thick clean zone and is marked at 3505 m (Fig. 4.4) and the deflection observed is equivalent to +19 mV. Log interpretation charts (Gen-6, SP-1 and SP-3) were used for interpretation.

Table 5.1. Rw calculation using SP method.

SSP	Rmf @ Fm. Temp	Rmfeq	Rweq	Rw (ohm.m)
+19 mV	0.028	0.024	0.04	0.042

5.2.6 Calculation of hydrocarbon and water saturation (Sh)

Saturation of hydrocarbons was calculated using formula which is

$$Sh = 1 - Sw$$

Saturation of water was calculated using formula which is

$$Sw = 1 - Sh$$

The value is multiplied with 100 to represent in percentage.

5.3 Marked prospect zones of interest

The zones of interest in Miano wells are identified on the basis of stable values of caliper log, high values of resistivity log with LLD higher than MSFL and LLS logs. Crossover between neutron and density log and lower values of sonic (DT) log. The well log interpretation of Miano wells is discussed below.

5.3.1 Prospect zone of interest marked in Miano-03 well

Prospect zone of interest was marked in Miano-03 well at the depth of 3304 m to 3310 in Lower Goru Formation (B sands) as shown in figure 5.1. The net thickness of B sand (reservoir) is 5.7 meters, well logs indicates a channel sand body as indicated by sharp base and top gamma ray peaks. Bulk density and neutron porosity gives a cross over in identified zone of interest depicting a gas zone along with GR log curve remain near 30 API which indicates the presence of sandstone lithology figure 5.2. Although, resistivity curves show separation between MSFL and LLD. Bulk density and neutron porosity cross over was also observed for the demarcation of this zone as a prospect zone. The results of the petrophysical interpretation of Miano-03 well is given below in table 5.2.

Table 5.2. Results of petrophysical interpretation of well Miano-03

Zone	Parameters					
	Net pay (m)	Vshale (% age)	Effective Porosity (% age)	Average Porosity (% age)	Saturation of water (% age)	Saturation of hydrocarbons (% age)
B Sand	6	28	14	20	30	70

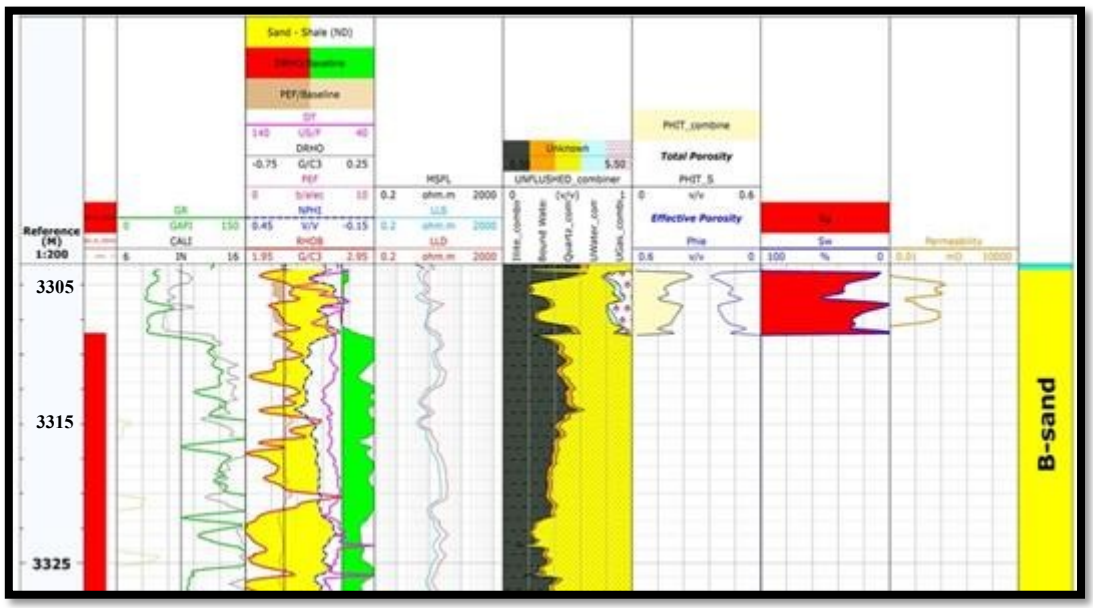

Figure 5.2. Petrophysical analysis of well Miano-03

5.3.2 Prospect zone of interest marked in Miano-04 well

Prospect zone of interest with net pay thickness of 5 meters was marked in Miano-04 well at the depth of 3326 – 3332 m in Lower Goru Formation (B sands) as shown in figure 5.2 Porosity is calculated using sonic log where data is affected by bad hole condition. MSFL, LLS and LLD resistivity curves shows separation in order MSFL < LLS < LLD, depicts hydrocarbon presence. Bulk density and neutron porosity also shows a cross over in identified zone of interest depicting the presence of gas zone along with sonic log curve suddenly goes left of scale at the start of zone of interest depicting interval transit time of acoustic waves decreases in hydrocarbon zone and GR log curve remain near 30 API which indicates the presence of sandstone lithology figure 5.3. The results of the petrophysical interpretation of Miano-04 well is given below in table 5.3.

Table 5.3. Results of petrophysical interpretation of well Miano-04

Zone	Parameters					
	Net pay (m)	Vshale (% age)	Effective Porosity (% age)	Average Porosity (% age)	Saturation of water (% age)	Saturation of hydrocarbons (% age)
B Sand	6	7	13	18	31	69

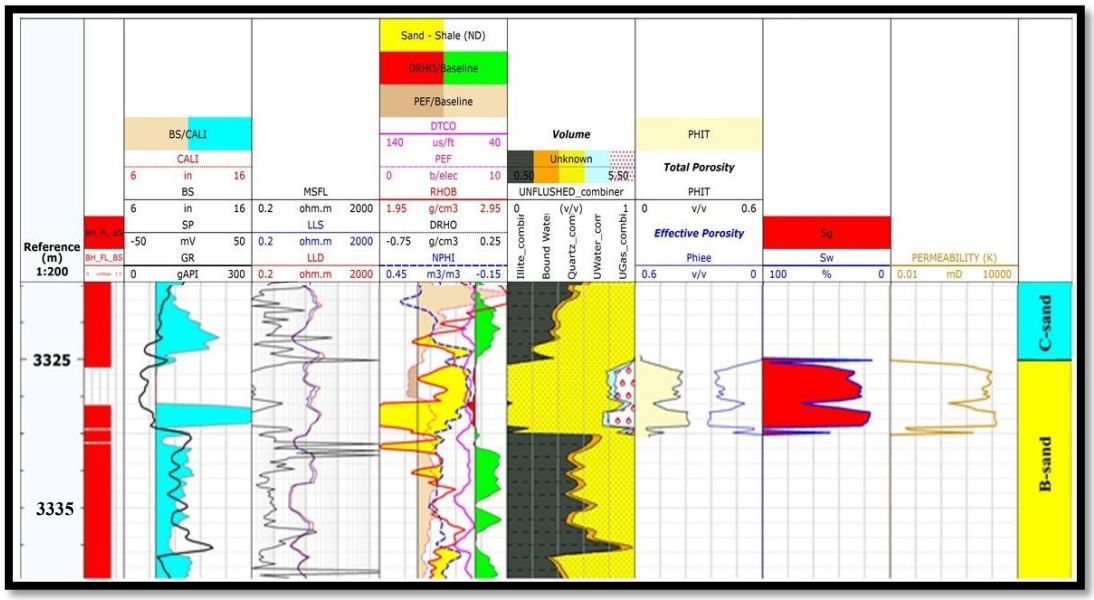

Figure 5.3. Petrophysical analysis of well Miano-04

5.3.3 Prospect zone of interest marked in Miano-09 well

Prospect zone of interest with 9 meter net pay thickness was marked in Miano-09 well at the depth of 3338 – 3347 m in Lower Goru Formation (B sands) as shown in figure. MSFL, LLS and LLD resistivity curves shows separation in order MSFL < LLS < LLD, depicts hydrocarbon presence. Bulk density and neutron porosity also shows a cross over in identified zone of interest depicting the presence of gas zone along with sonic log curve suddenly goes left of scale at the start of zone of interest depicting interval transit time of

acoustic waves decreases in hydrocarbon zone and GR log curve remain near 25 API which indicates the presence of sandstone lithology figure 5.4. B sand represents a tidal channel sand body as evident by log signatures. Reservoir quality in this well is excellent as evident from petrophysical analysis, furthermore permeability can be related to directly to porosity indicating that the reservoir was deposited in high energy condition where the fines were washed out thus providing shale clean sand. The results of the petrophysical interpretation of Miano-09 well is given below in table 5.4.

Table 5.4. Results of petrophysical interpretation of well Miano-09

Zone	Parameters					
	Net pay (m)	**Vshale (% age)**	**Effective Porosity (% age)**	**Average Porosity (% age)**	**Saturation of water (% age)**	**Saturation of hydrocarbons (% age)**
B Sand	9	12	14	19	28	72

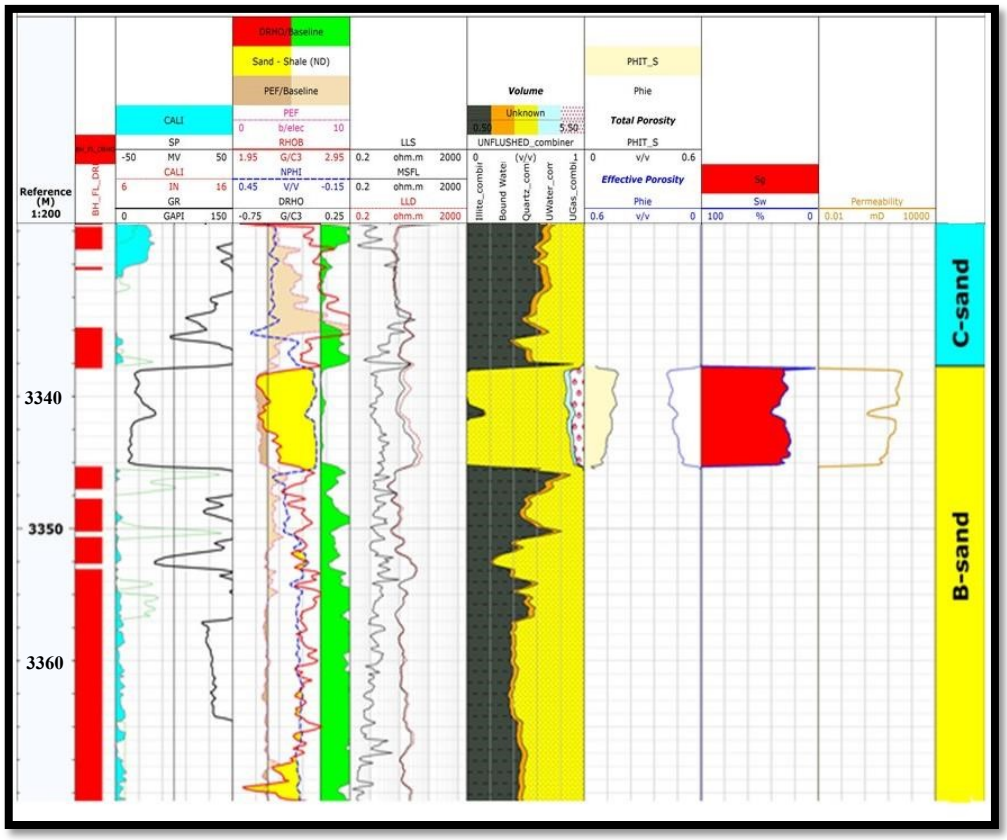

Figure 5.4. Petrophysical analysis of well Miano-09

CHAPTER 6

SEISMIC DATA INVERSION AND POROSITY PREDICTION

6.1 Introduction to seismic inversion

Subsurface physical properties can be estimated by observed geophysical data in a technique known as geophysical inversion. If seismic data is used for this purpose, then it is known as seismic inversion. Seismic data is used as an input for determining earth's physical properties and usually sonic and density logs, seismic data volume and series of interpreted horizons are typical data sets that are used as input data sets for post stack seismic inversion projects. If this seismic inversion is applied after stack, then it is known as post stack seismic inversion and if it is applied on the data that is not stacked with multi offset assumption then it is known as pre-stack seismic inversion.

Post stack seismic inversion holds a zero-offset assumption applied normally on processed stacked data, normally known as seismic inversion or acoustic impedance inversion. Reservoir properties across the reservoir can be predicted from a resulting impedance volume, away from well control. Post stack impedance inversion can prove helpful for determination of lithology and fluid content distribution which are important for reservoir characterization and subsequent reservoir management. In this research work acoustic impedance model got generated from seismic data set of different 2-D seismic lines. One of the major benefits of seismic inversion is substantial enhancement in the seismic resolution (Veeken, 2007). Seismic inversion uses the seismic and well log data which allows the extraction of subsurface geology in terms of lithology, pore fluid presence and extraction of lithologic parameters such as porosity, volume of shale and water saturation of entire area beyond the well control (Veeken, 2007).

Acoustic impedance contrast tends to comprehend the geological boundaries, so that a relationship can be established between acoustic impedance contrast and reservoir characteristics for demarcation of sweet spots.

6.2 Objective of seismic inversion

The principle objective of seismic inversion is to transform seismic reflection data into a quantitative rock property, descriptive of the reservoir. In its most simple form, acoustic impedance logs are computed at each CMP which simple means if we had drilled and logged wells at the CMP's what would the impedance logs have looked like? Compared to working with seismic amplitudes, inversion results show higher resolution and support more accurate interpretations. This in turn facilitates better estimation of reservoir properties such as porosity and net pay. An additional benefit is that interpretation efficiency is greatly improved, more than offsetting the time spent in the inversion process (Veeken, 2007).

6.3 Benefits of seismic inversion

Benefits of seismic inversion include compensation for and reduction of the effects of wavelet tuning, presentation of output as geologic layers rather than reflection edges, merging of known low frequency geologic and geophysical information with seismic data, modelling and inclusion of layer stratigraphy, inclusion of geophysical constraints from known information or analogues, calibration to well log data, improved interpretability of seismic horizons, increased bandwidth in the inversion output, attenuation of random noise (Veeken, 2007).

6.4 Model based inversion

In a model-based inversion, a simple initial acoustic impedance model is convolved with the wavelet to obtain a synthetic response that is compared with the actual seismic trace. The acoustic impedance model is altered iteratively until the difference between the inverted trace and the seismic trace is reduced to a threshold value. A model with a very small difference is accepted as a solution. An advantage of model-based inversion is that it gives satisfactory results, even with limited well control and poor quality seismic. The seismic dataset itself acts as the guide for inversion and a wavelet can be easily derived straight from the seismic. The least squares inversion method is a type of model-based inversion where the threshold value is the smallest least-squares error (Veeken, 2007).

6.5 Methodology adopted for seismic inversion

'STRATA' is the module used in Hampson Russel software for both pre-stack and post stack inversion. In post stack seismic inversion, HRS inputs post stack seismic volume along with well data and outputs an acoustic impedance volume. The type of post stack seismic inversion which is run over the research area is model-based inversion. The methodology adopted for post stack seismic inversion in Hampson Russel software is as follows:

'Geoview' is the application of Hampson Russel software for initiating all the modules of HRS. Seismic and well data were uploaded in it by the means of 'Well Explorer' module. This loaded will now then be available for 'STRATA' to perform inversion processes.

Since the objective of this research work is the application of model based inversion for the computation of porosity at level of B-Sands. Therefore for this very purpose complete log suite of Miano-04 and Miano-09 wells along with seismic velocity functions of well line SP2092-115 and SP2092-123 were loaded in module 'Well Explorer'.

The next step was to open the project in 'STRATA'. All the interpreted horizons namely; top Lower Goru Formation, Top of D interval, Top of C interval, Top of B interval were imported from Geographix in 'STRATA' module. First of all the conditioning of well log data of Miano-04 and Miano-9 was carried out to remove errors from the well log. The errors in the well log data could be because of caving and swelling of well formations. The errors are removed from the well logs to get good inversion results as shown in figure 6.1 and figure 6.2

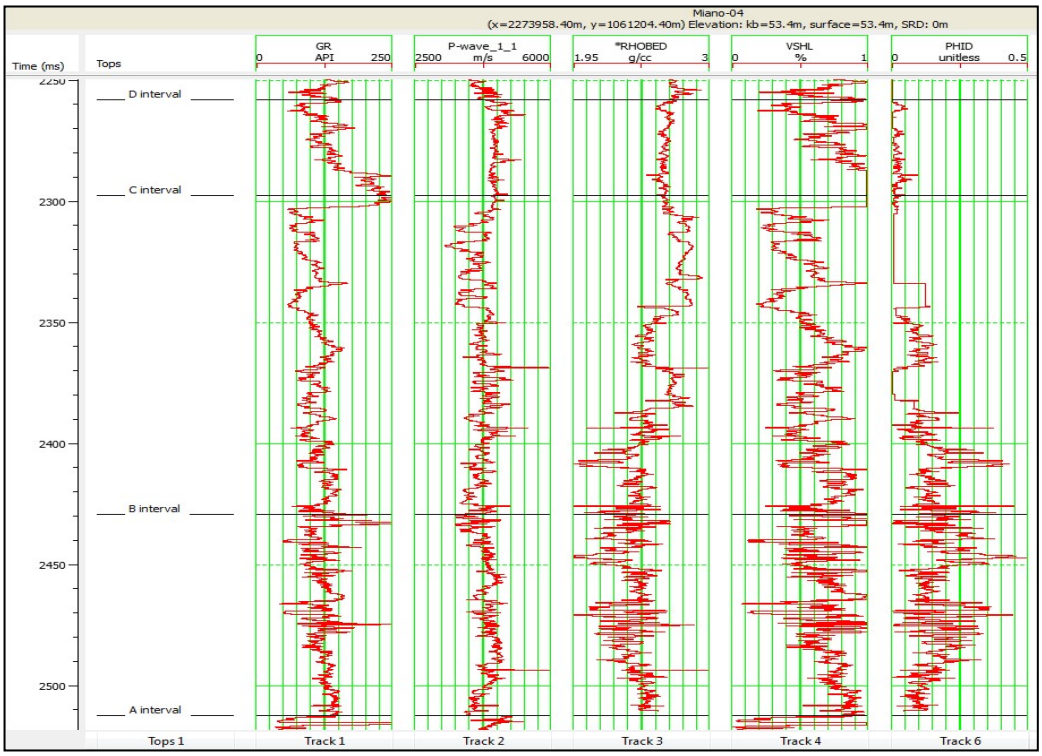

Figure 6.1. Conditioned well log data of well Miano-04

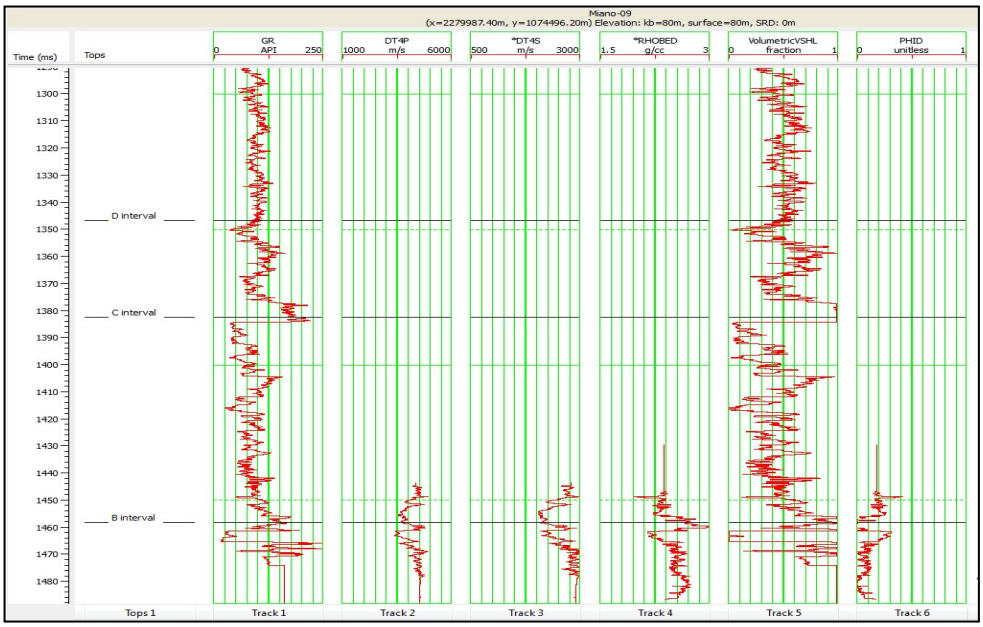

Figure 6.2. Conditioned well log data of well Miano-09

After well log conditioning the next task is to perform the cross-plot analysis. The cross-plot analysis was carried out to define the parameter on the basis of which reservoir sands, tight sands and shales lithology could be segregated from each other. The cross-plot analysis helped in defining the most suitable variables for segregation of these lithologies. The cross-plot analysis showed that reservoir sands of B-interval could be separated with low density and low P-impedance as displayed in figure 6.3 and figure 6.4. While segregation between shales and tight sands is quite difficult on the basis of Pimp and density.

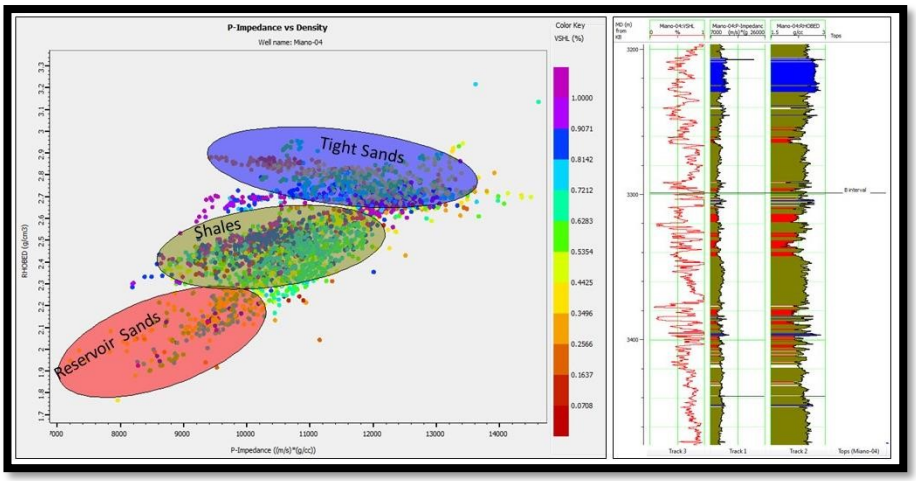

Figure 6.3. Cross-plot analysis for Miano-04 well

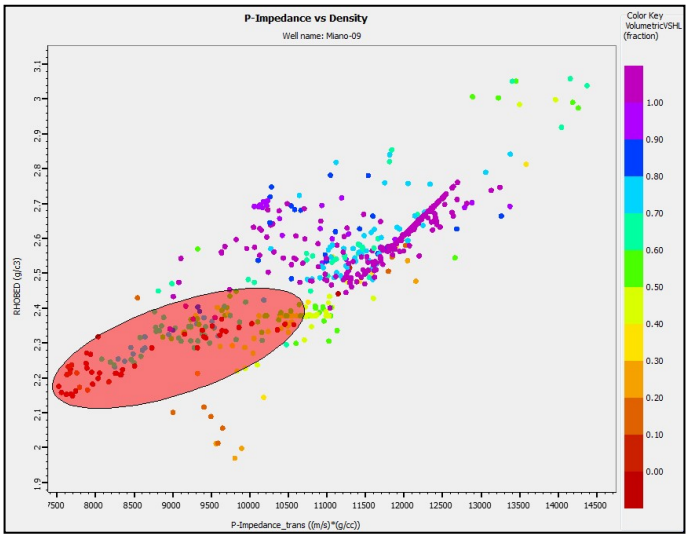

Figure 6.4. Cross-plot analysis for Miano-09 well

The next step is well to seismic tie and extraction of seismic wavelet. Statistical wavelet was extracted using seismic data only, after importing the horizons. Extracted statistical wavelet got displayed in both time and frequency domains with spectrum threshold 20%, operator length 200 samples and taper length 50 samples as displayed in figure 6.5 and figure 6.6.

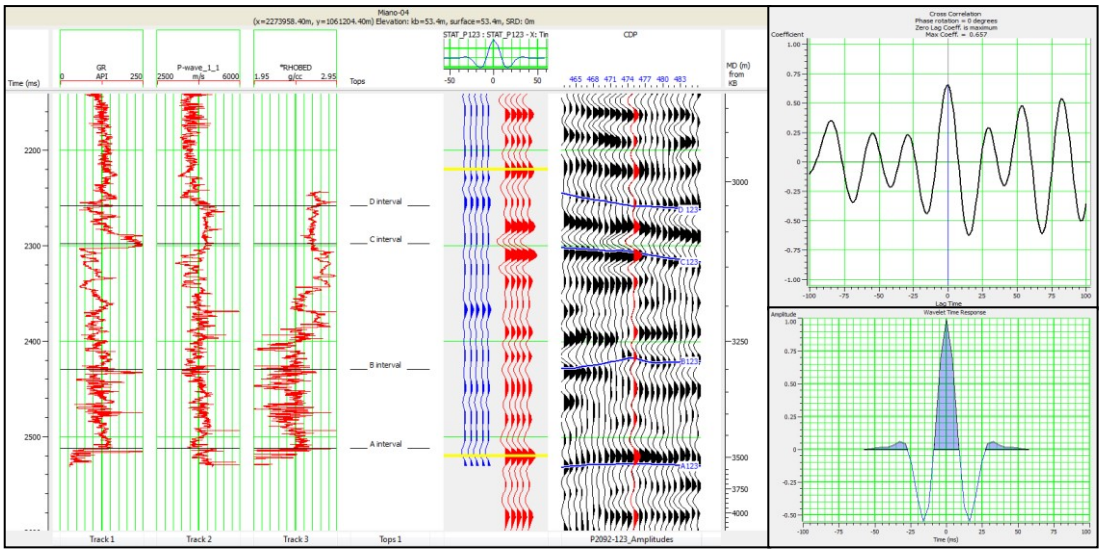

Figure 6.5. Seismic to well tie and extracted statistical wavelet forMiano-04 well

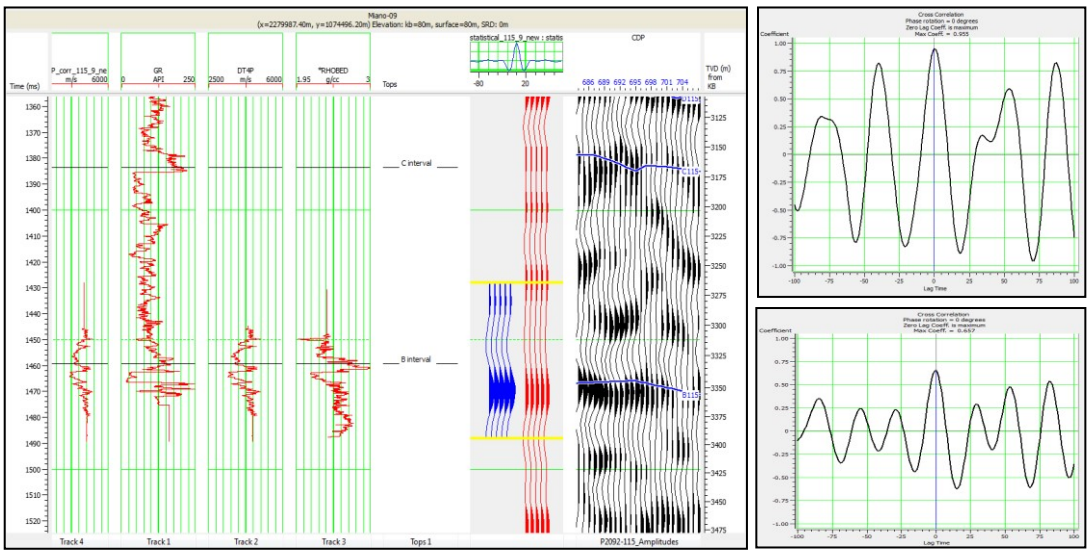

Figure 6.6. Seismic to well tie and extracted statistical wavelet for Miano-09 well

The next step was to build an initial model which was a low frequency model post stack seismic inversion generates an acoustic impedance volume

only for which P-wave impedance got generated from sonic and density log (for acoustic impedance inversion). In the same manner, initial velocity model was generated using velocity functions with information of time and velocity as displayed in figure 6.7 and figure 6.8.

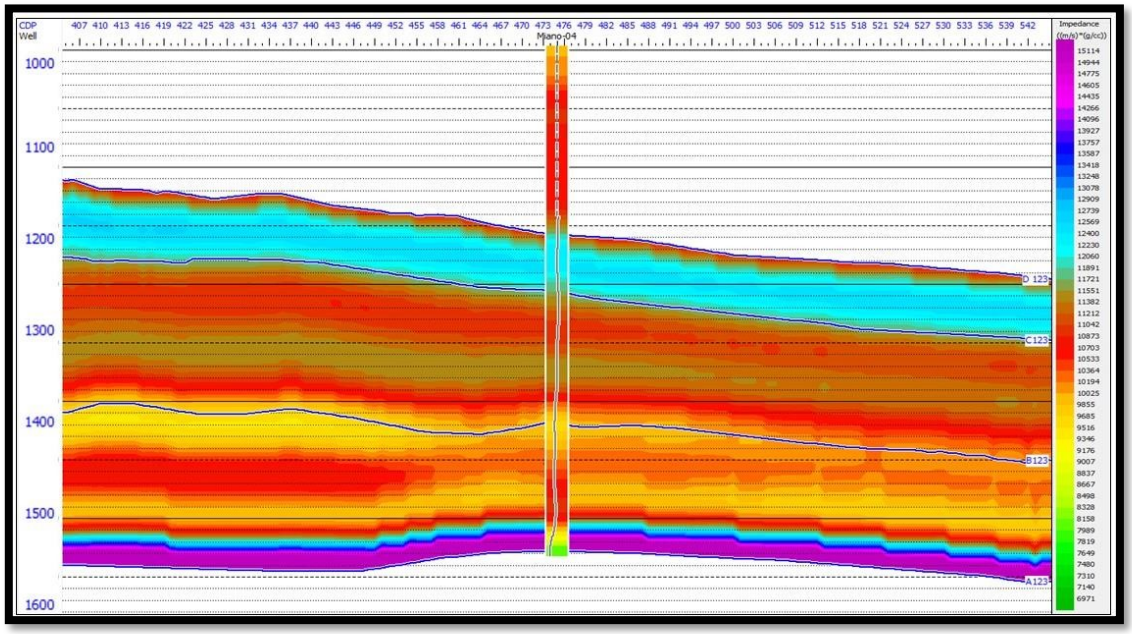

Figure 6.7. Low frequency model at Miano-04 well location

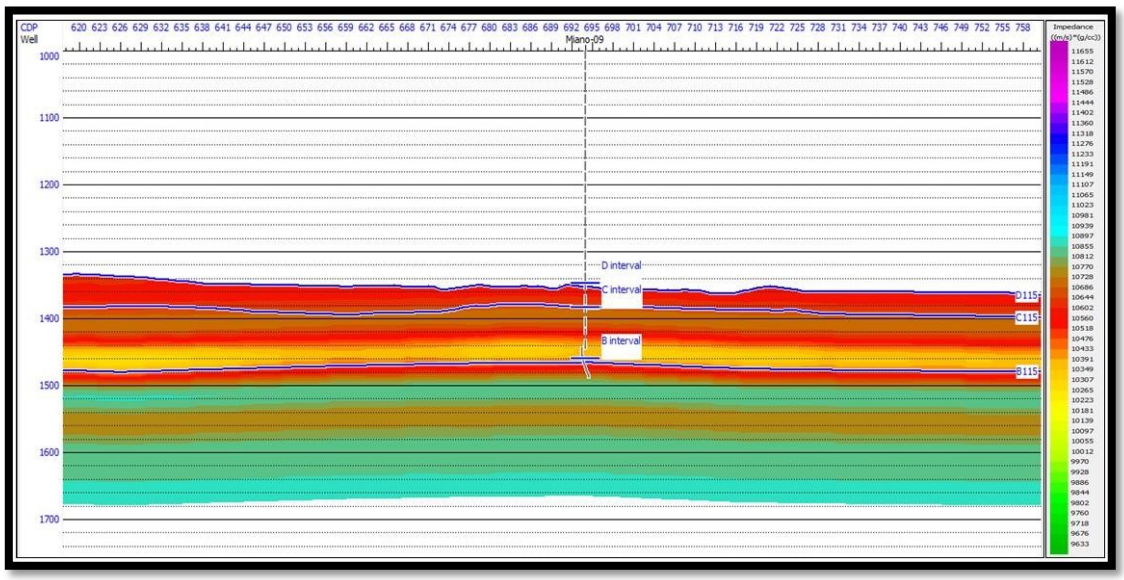

Figure 6.8. Low frequency model at Miano-09 well location

Low frequency data provides deeper penetration useful for imaging deep targets, and provides greater stability in inversion. Broader bandwidths produce sharper detailed definition. Both low and high frequencies are required for high-resolution imaging of important shallow features such as thin beds and small sedimentary traps. Since the seismic trace lacks a low frequency velocity trend because of the band-limited wavelet, the inverted trace lacks the "excursions" seen on the original sonic log. Therefore low frequency component must be added from the geological model.

The next step is to perform post stack inversion analysis. The generated seismogram was extrapolated on both sides of the well. The difference between generated synthetic and original seismic section is known as Objective function. Therefore iterations are run for as much times that the difference between synthetic and original seismic become minimum. The correlation coefficient at Miano-04 well location comes out to be 0.9930, while the correlation coefficient for Miano-09 comes out to be 0.9865 with the error of 0.119312 and 0.164097 respectively. The results of post stack inversion analysis are displayed in figures 6.9 and 6.10 respectively.

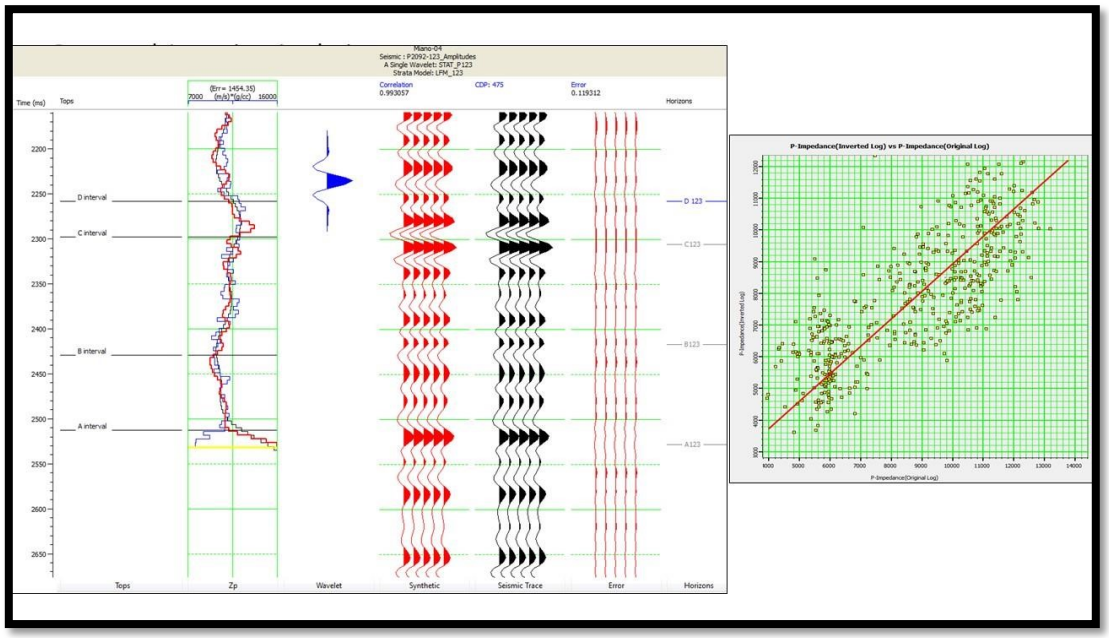

Figure 6.9. Post stack inversion analysis at Miano-09 well location

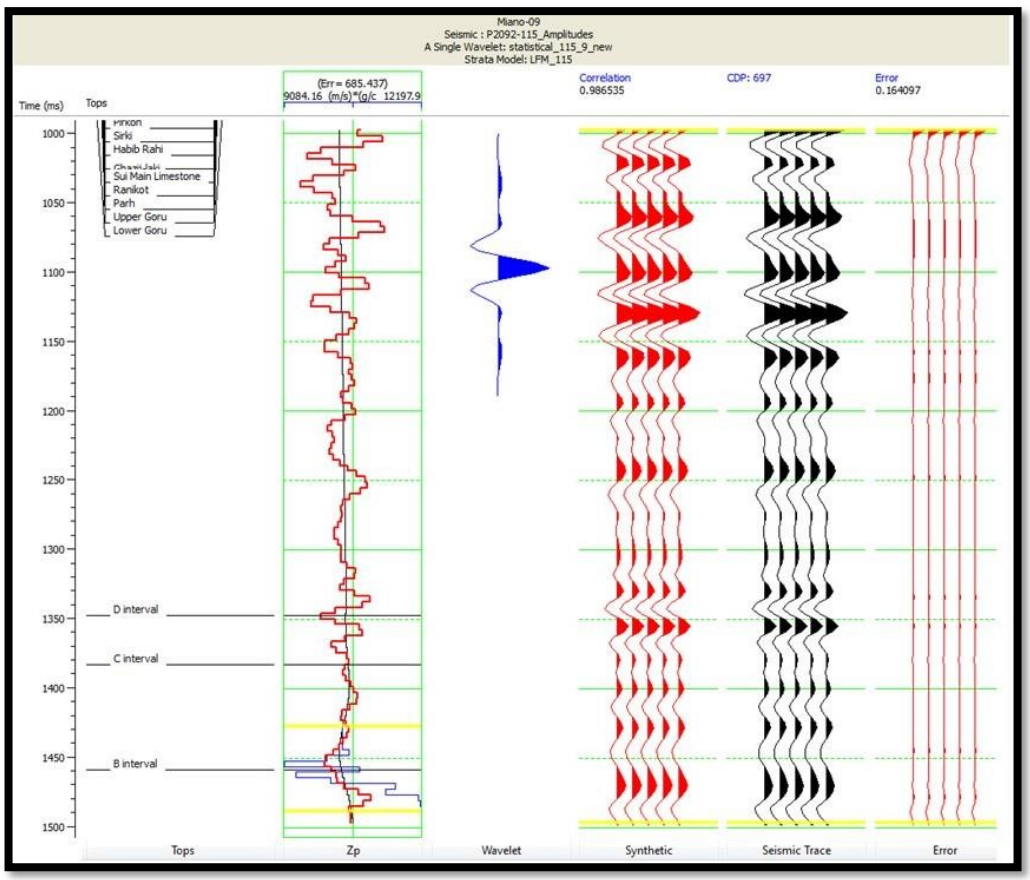

Figure 6.10. Post stack inversion analysis at Miano-09 well location

The next step was to perform model based inversion. Seismic inversion is required to perform over this original acquired seismic data set. After generating a statistical wavelet, seismic curve data was inserted (inserted curve data; P-wave) in 'STRATA' module of CGG Hampson Russel Suite. The result of entire activity was an inverted seismic section which gives us information in the form of acoustic impedance contrast. Interpreted horizons also displayed over it. This inverted seismic section can be interpreted in terms of variations in subsurface geology like changes in lithology etc. and to develop its relationship with reservoir characteristics as displayed in figure 6.11.a, 6.11.b and 6.12. Only control line with Miano-04 and Miano-09 well locations are focused for seismic inversion in this research work because of seismic and well data limitation.

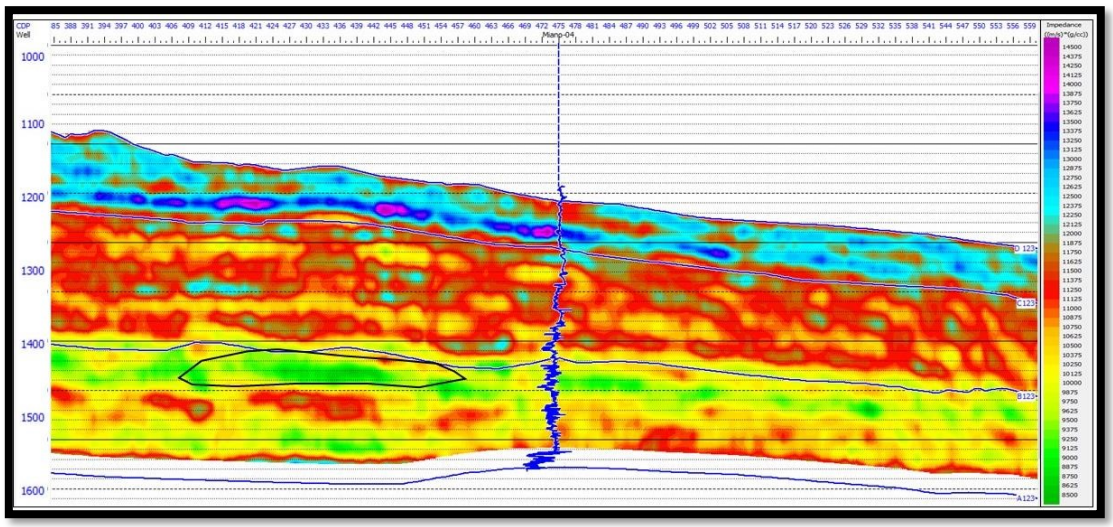

Figure 6.11.a. Results of Model based inversion at Miano-04 well location with inserted P- wave curve data

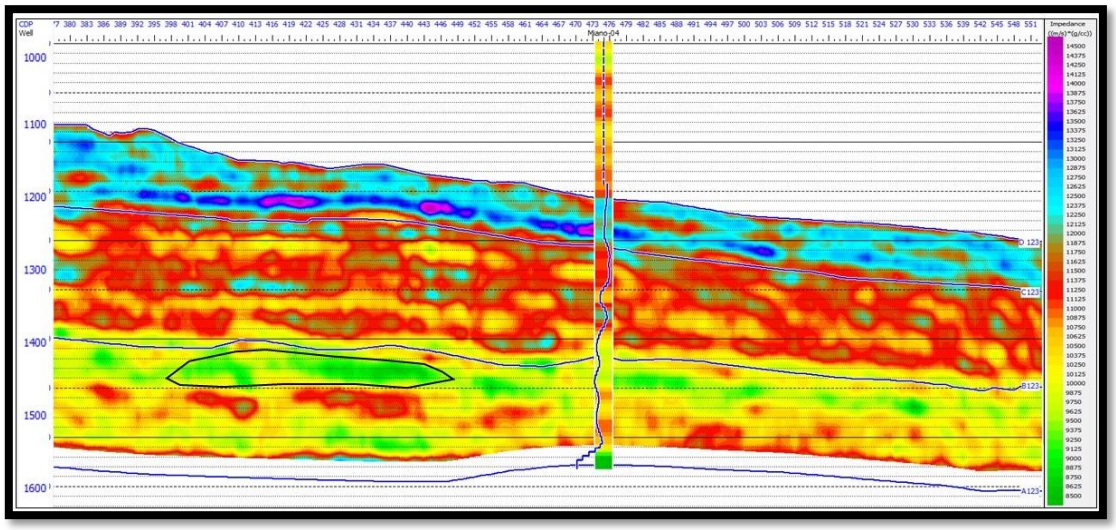

Figure 6.11.b. Results of Model based inversion at Miano-04 well location with inserted impedance data

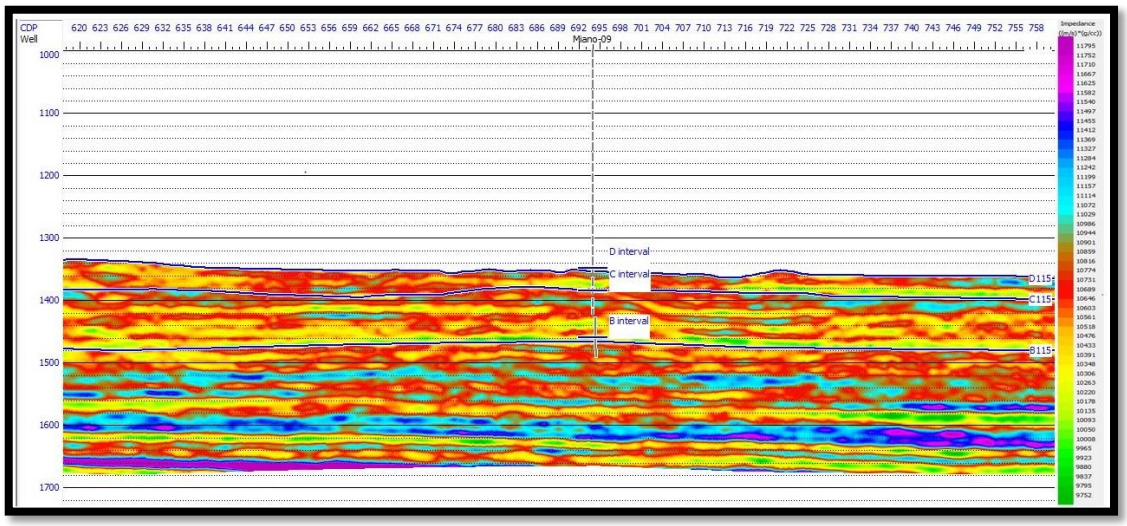

Figure 6.12. Results of Model based inversion at Miano-09 well location

By applying model based inversion it is possible to generate a porosity section for porosity prediction in the area for Lower Goru sand members. A linear relationship between porosity and acoustic impedance was built based on the wire-line logs from existing wells Miano-4 and Miano-9. From this plot the following equation was derived:

$$Y = m\,(AIMP) + c$$

Where y is the porosity, m is the slope, AIMP is the acoustic impedance, and c is the intercept. The equation was obtained as a regression line for the clean sands as shown in figure 6.13 and 6.14. The obtained correlation between porosity and acoustic impedance for Miano-4 and Miano-9 well location is 74.1% and 81.11% respectively.

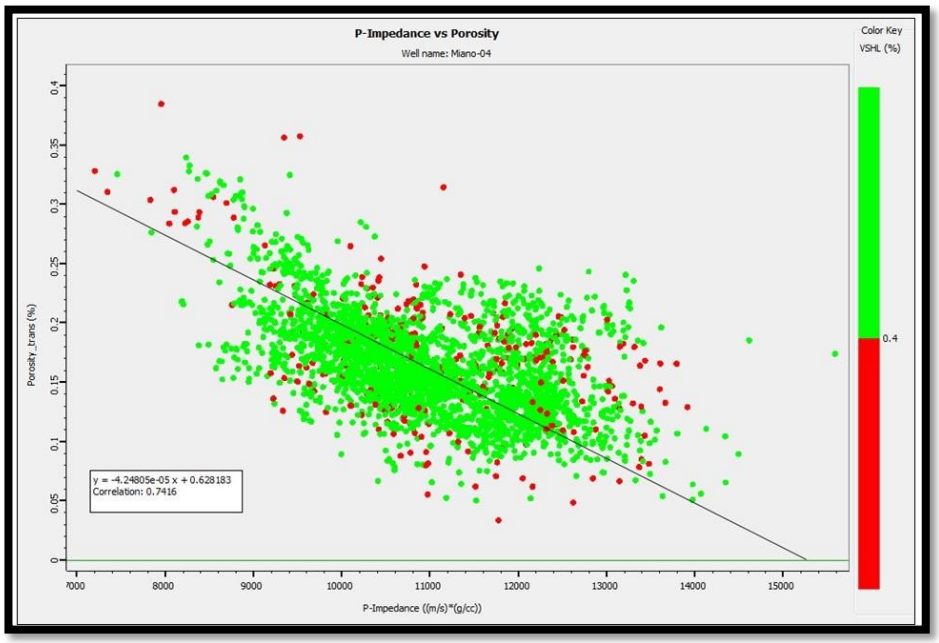

Figure 6.13. Cross-plot between porosity and P-impedance at Miano-04 well location

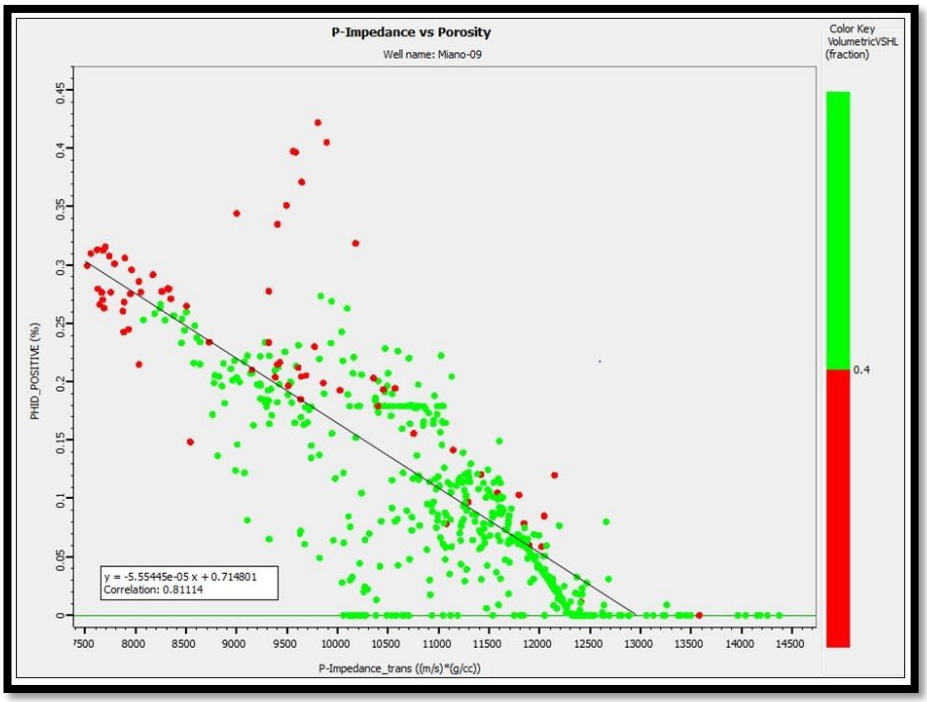

Figure 6.14. Cross-plot between porosity and P-impedance at Miano-09 well location

Then above equations have been applied to the available relative acoustic impedance section and a porosity sections have been obtained at Miano-04 and Miano-09 well locations. The correlation coefficient for B-sand is 74.16% and 81.11% at Miano-04and Miano-09 well locations respectively. On the basis of excellent correlation from the regression equation, acoustic impedance is used to compute the porosity of B sands over the section as illustrated in figures 6.15 and 6.16.

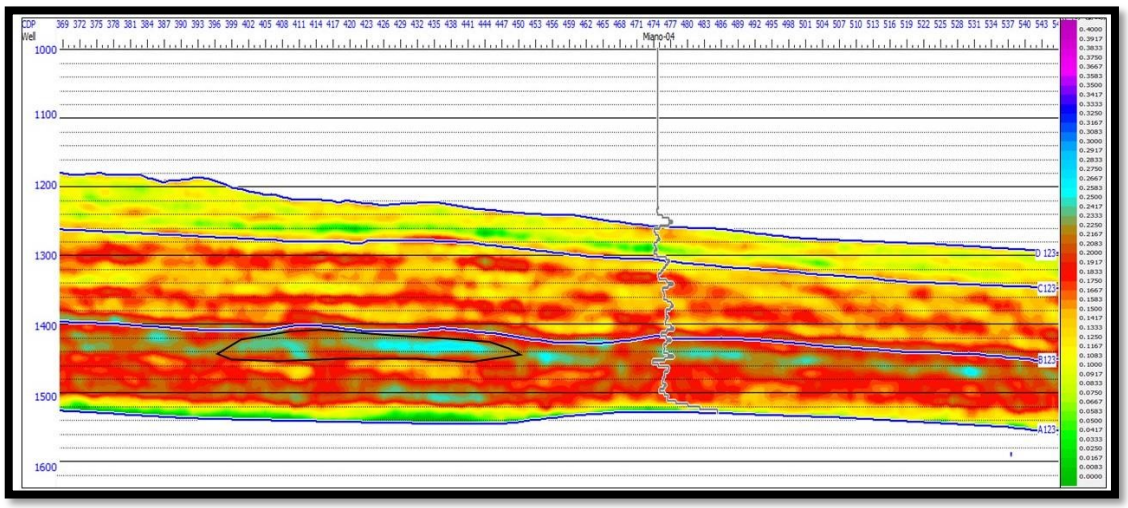

Figure 6.15. Porosity modeling from P-impedance at Miano-04 well location

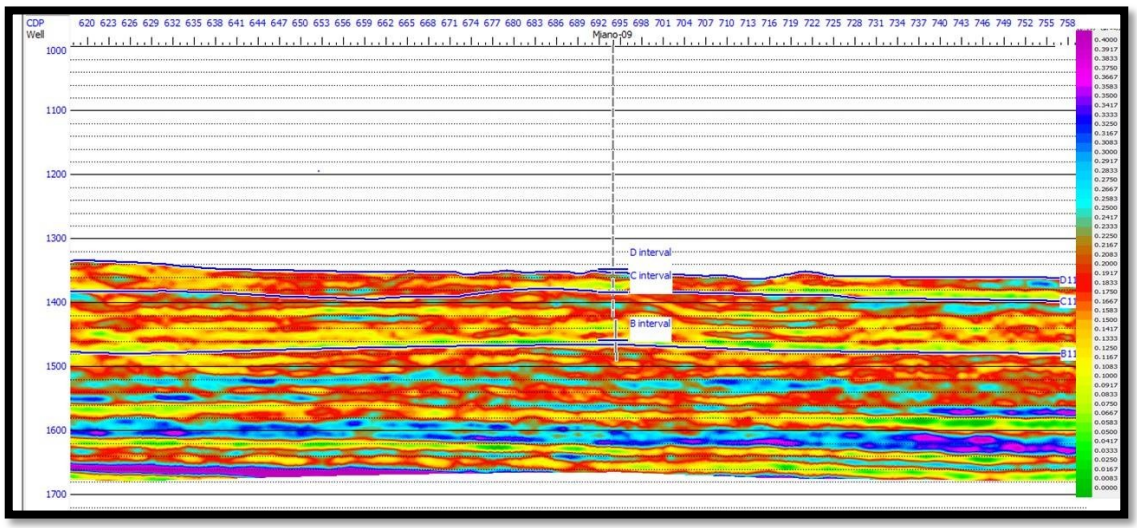

Figure 6.16. Porosity modeling from P-impedance at Miano-09 well location

The average porosity value of B-sands computed from petrophysical analysis is 18%. While the value of porosity computed from P-impedance falling in the range of 18 – 20%. Similarly the average porosity computed from petrophysical analysis at Miano09 well location is 19%. The porosity modeled from acoustic impedance is falling in the range of 15 – 18%. These results are thus validating the lateral porosities computed for B-sands using model based seismic inversion.

DISCUSSION

Geophysical techniques like; seismic interpretation, petrophysical analysis, seismic attribute analysis and seismic inversion were conducted on Miano area and following deliberation can be made after analyzing the results of these geophysical techniques:

Seismic interpretation has confirmed the presence of trans-tensional tectonics as negative flower structure along with horsts, normally faulted grabens and tilted fault blocks are present with two-way dip closure at the level of Lower Goru B Sands in Miano area. Petrophysical analysis of Miano-03, Miano-04 and Miano-09 wells has shown at least one promising reservoir zone at Lower Goru B Sands level in each well, confirming Lower Goru B Sands as a proven hydrocarbon reservoir in Miano area. Promising reservoir zone in Miano-03 well has shown 70 % hydrocarbon saturation Bad hole quality has also effect the results of petrophysical interpretation. Promising reservoir zone in Miano-04 well has shown 69% hydrocarbon saturation. Promising reservoir zone in Miano-09 well has shown 72% hydrocarbon saturation. Seismic attributes like instantaneous amplitude Instantaneous phase, instantaneous frequency, variance attribute and shale indicator atrributes have proved useful in detecting major lithological discontinuities, bright spots, faults, fractures and bed thickness identification along with lithological response to these applied seismic attributes. These attributes suggests that the thickness of Lower Goru B Sands decreased with an increase in frequency suggesting an idea regarding bed thickness and channel characterization of Lower Goru B Sands. Seismic inversion techniques like; model based inversion, colored inversion and velocity inversion have proved successful in providing insight regarding porosity and lithological content, especially of Lower Goru B Sands reservoir. Acoustic impedance contrast with color variation depicts changes in lithological content at different level of reservoir horizons. Model based inversion at the level of Lower Goru B Sands reveals that sweet spots can be marked in eastward direction with low acoustic impedance contrast and high porosity trend. Porosity

extracted from inverted seismic section suggests ~18% of total porosity at the level of Lower Goru B Sands.

CONCLUSIONS

Following conclusions can be drawn from this research based on seismic interpretation, petrophysical analysis, seismic attribute and seismic inversion analyses:

a. Seismic sections and contour maps depicts negative flower structure (strike slip component) along with horsts, normally faulted grabens and tilted fault blocks with two way dip closure at the level of Lower Goru B Sands. NW-SE trending faults have played a vital role in compartmentalization of a reservoir.

b. Petrophysical analysis showed that atleast one reservoir zone of significant thickness and hydrocarbon saturation in each Miano well is potentially good enough to produce commercially.

c. Clear zones of sand bodies with channel geometries are indicated by various attributes. Presence of bright spots in eastward direction demarcated by instantaneous amplitude attribute at the level of Lower Goru B Sands makes it a potential reservoir formation of Miano area.

d. Seismic inversion techniques clearly enhanced the sweet spots in eastward direction at Lower Goru B Sands level which is reliable for further development of this field, which depicts the potential zone at level of Lower Goru B sands.

REFERENCES

Ahmed, R, Ali. M. and Ahmad, J., 1994. Review of Petroleum occurrence and Prospects of Pakistan with special reference to adjoining Basins of India, Afghanistan and Iran. Pakistan Journal of Hydrocarbon Research, no. 6, 1-2.

Ahmad N., Fink P., Sturrock S., Mahmood T., Ibrahim M., 2012, "Sequence Stratigraphy as Predictive Tool in Lower Goru Fairway, Lower and Middle Indus Platform, Pakistan"., Adapted from Pakistan Association of Petroleum Geoscientists (PAPG), Annu. Tech. Conf. (ATC), Islamabad, Pakistan, October 8-9.

Ahmad, S., Ullah, M., Ullah, S., Khan, S., Khan, Y., Jan, I.U., Rehman, K., Mohibullah, M., Attaulllah and Jan, S., 2018. Stratigraphic and Paleoclimatic Reconstruction of the Upper Carboniferous-Lower Permian strata from the Southern Gondwanaland remnants in Pakistan. STRATIGRAPHY, 15(2), pp.69-90.

Bregar, B. U., Zafar, N., Ahmad, T., Aftab, M.N., Murtaza, G. and Rehman, A. M.N., 2008. Continuous WGR measurement in production testing with multiphase Flow Meter in Miano Gas Field. PAPG-SPE Annual Technical Conference, 276.

Brown, A.R., 2001. Understanding seismic attributes. Geophysics, 66(1), pp.47-48.

Brown, A.R., 2011. Interpretation of Three-Dimensional Seismic Data: AAPG Memoir 42, /SEG Investigation in Geophysics, No. 9 (Vol. 42). AAPG.

Chopra, S. and Marfurt, K., 2006. Seismic Attributes–a promising aid for geologic prediction. CSEG Recorder, 31, pp.110-120

Dobrin MB, Savit, CH 1988. Introduction to Geophysical Prospecting, 4th

Edition. McGraw-Hill Book Company, 867 pp

Ebdon C., Wasimuddin M., Malik A.H., Akhter S., 2004, Sequence stratigraphy of the B Sand (upper sand, Lower Goru Formation) in the Badin area: Implication for development and exploitation. Annu. Tech. Conf., Islamabad, Pakistan.

Iqbal S, Jan UI, Hanif M, 2014. The Mianwali and Tredian Formations: an example of the Triassic Progradational Deltaic System in the low-latitude western Salt Range, Pakistan. Arab J Sci Eng 39(7):5489–5507. doi:10.1007/s13369-013-0836-2

Jadoon, I.A., Hinderer, M., Wazir, B., Yousaf, R., Bahadar, S., Hassan, M. and Jadoon, S., 2015. Structural styles, hydrocarbon prospects, and potential in the Salt Range and Potwar Plateau, north Pakistan. Arabian Journal of Geosciences, 8(7), pp.5111-5125.

Kemal A., Zaman A.S.H., Humayon M., 1991, New directions and strategies for accelerating petroleum exploration and production in Pakistan. Proceedings, International Petroleum Seminar, Islamabad, Pakistan, 16–57.

Kemal, A., 1992, Geology and new trends for hydrocarbon exploration in Pakistan, in Ahmed, G., Kemal, A., Zaman, A.S.H., and Humayon, M., eds., New directions and strategies for accelerating petroleum exploration and production in Pakistan: Proceedings, international petroleum seminar, November, 22–24, 1991: Islamabad, Pakistan, Ministry of Petroleum and Natural Resources, p. 16–57.

Kazmi, A.H. and Jan, M.Q., 1997. Geology and tectonics of Pakistan. Graphic publishers.

Khan, M.R., Iqbal, M., Ahmad, A., Murtaza, G., and Khan, W.A., 2013. An Integrated Approach for Assessment of Lower Goru Reservoir Quality in Western Part of Badin Area, Lower Indus Basin, Pakistan. PAPG/SPE Annual Technical Conference 2013, Islamabad, Pakistan. This publication is only available in digital format provided to the participants only

Krois, P., Mahmood, T. and Milan, G., 1998, November. Miano field, Pakistan, A case history of model driven exploration. In Proceedings Pakistan Petroleum Convention (Vol. 98, pp. 112-131).

Petro-consultants, 1996, Petroleum exploration and production digital database: Petroconsultants, Inc., [P.O. Box 740619, 6600 Sands Point Drive, Houston TX 772740619, U.S.A. or Petroconsultants, Inc., P.O. Box 152, 24 Chemin de la Mairie, 1258 Perly, Geneva, Switzerland]. Powell, C. M.A., 1979

Petro-consultant, 2000, Petroleum exploration and production digital database: Petroconsultants, Inc., [P.O. Box 740619, 6600 Sands Point Drive, Houston TX 772740619, U.S.A. or Petroconsultants, Inc., P.O. Box 152, 24 Chemin de la Mairie, 1258 Perly, Geneva, Switzerland]. Powell, C. M.A., 1979

Qadri, I. B., 1995. Petroleum Geology of Pakistan, Pakistan Petroleum Limited, 30, 87, 88, 95p.

Raza et al., 1990 Raza H.A., Ali S.M., Ahmed R., 1990, Petroleum geology of Kirthar sub-basin and part of Kutch Basin. Pak. J. Hydro. Res. 2, 1, 29–73.

S.M.I. Shah, Stratigraphy of Pakistan", The Geological Survey of Pakistan Memoirs, pp. 12, 30, 73, 89, 1977

Siguaw, S.G., Estes-Jackson, J.E., Ingraham, S.E. and Shewmake, D.W., 2001. An integrated 3-D reservoir characterization at Riverton Dome Field, Wyoming. The Leading Edge, 20(11), pp.1226-1238.

Subrahmanyam, C., Gireesh, R., Chand, S., Raju, K.K. and Rao, D.G., 2008. Geophysical characteristics of the Ninetyeast Ridge–Andaman island arc/trench convergent zone. Earth and Planetary Science Letters, 266(1-2), pp.29-45.

Sampson, A., 2012. A seismic attribute study to assess well productivity in the Ninilchik field, Cook Inlet basin, Alaska.

Soleimani, F., Hosseini, E. and Hajivand, F., 2020. Estimation of reservoir porosity using analysis of seismic attributes in an Iranian oil field. Journal of Petroleum Exploration and Production Technology, pp.1-28.

Taner, A.H. and Brignell, J.E., 1997. Virtual instrumentation and intelligent sensors. Sensors and Actuators A: Physical, 61(1-3), pp.427-430.

Taner, M.T., 2001. Seismic attributes. CSEG recorder, 26(7), pp.49-56.PPL annual report, 2011

Veeken C.H., 2007. Seismic Stratigraphy, Basin Analysis and Reservoir Characterization. Handbook of Geophysical Exploration, Seismic Exploration 37.

Elsevier, Amsterdam. 522p.

Watters, M., 2008. The complementary nature of geophysical survey methods. In Seeing the unseen. Geophysics and landscape archaeology (pp. 209-226). CRC Press.

Wandrey, C.J., Law, B.E., and Shah, H.A., 2004. Sembar Goru/Ghazij Composite Total Petroleum System, Indus and Sulaiman-Kirthar Geologic Provinces, Pakistan and India. USGS Bulletin 2208-C, no. 2-10. This publication is only available online at: http://pubs.usgs.gov/bul/b2208-c/